iScience

CellPress
OPEN ACCESS

Article

Mixed-surface polyamidoamine polymer variants retain nucleic acid-scavenger ability with reduced toxicity

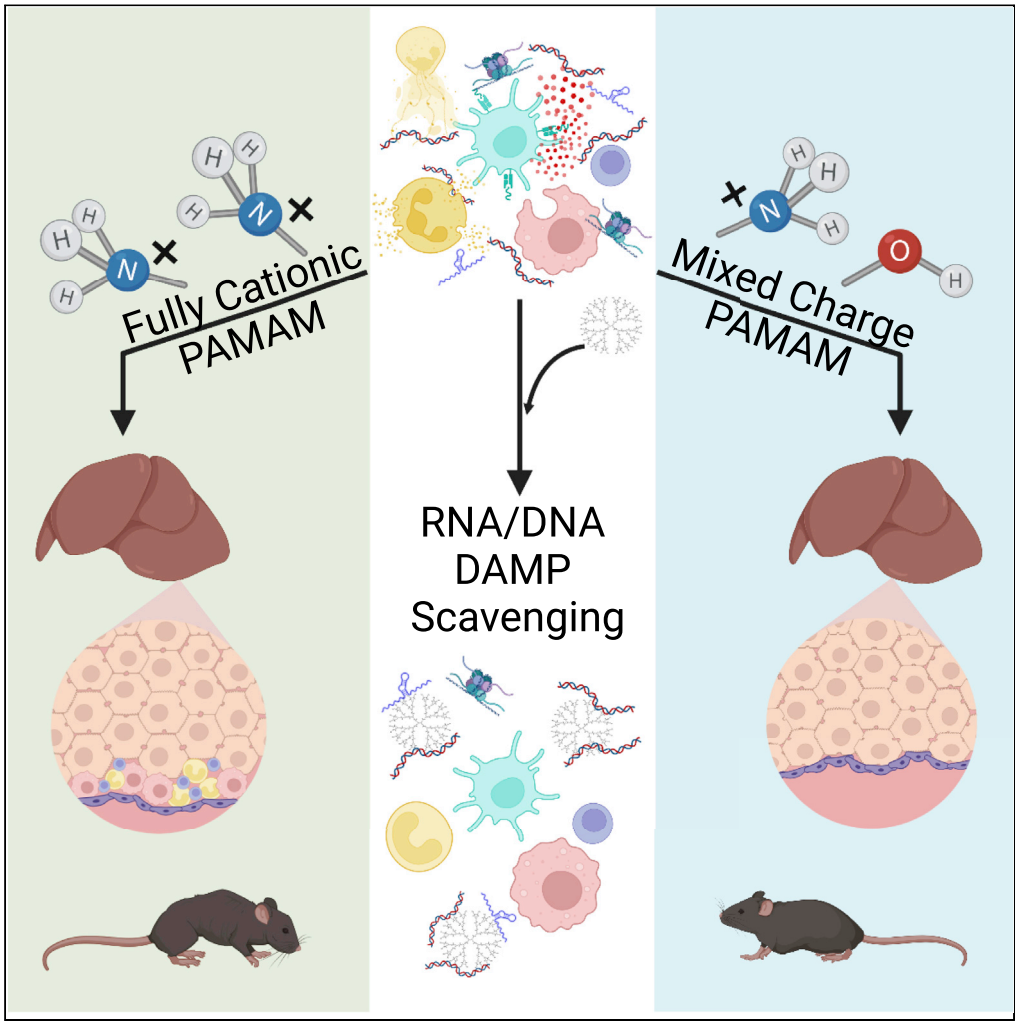

Lyra B. Olson, Nicole I. Hunter, Rachel E. Rempel, ..., David S. Pisetsky, Jeffrey I. Everitt, Bruce A. Sullenger

bruce.sullenger@duke.edu

Highlights

Mixed-surface PAMAM variants scavenge nucleic acid DAMPs without cellular toxicity

Variants induce less weight loss and serosal inflammation *in vivo* than PAMAM G3

The G3 50:50 variant reduces glomerulonephritis in lupus-prone MRL-*lpr* mice

Mixed-surface PAMAMs are a new class of scavengers with improved biocompatibility

Olson et al., iScience *25*, 105542
December 22, 2022
https://doi.org/10.1016/j.isci.2022.105542

iScience

CellPress
OPEN ACCESS

Article

Mixed-surface polyamidoamine polymer variants retain nucleic acid-scavenger ability with reduced toxicity

Lyra B. Olson,[1,2] Nicole I. Hunter,[1,3,10] Rachel E. Rempel,[1,10] Haixiang Yu,[1] Diane M. Spencer,[4] Cynthia Z. Sullenger,[1,5] William S. Greene,[6] Anastasia K. Varanko,[7] Seyed A. Eghtesadi,[7] Ashutosh Chilkoti,[7] David S. Pisetsky,[4,8] Jeffrey I. Everitt,[9] and Bruce A. Sullenger[1,2,7,11,*]

SUMMARY

Nucleic acid-binding polymers can have anti-inflammatory properties and beneficial effects in animal models of infection, trauma, cancer, and autoimmunity. PAMAM G3, a polyamidoamine dendrimer, is fully cationic bearing 32 protonable surface amines. However, while PAMAM G3 treatment leads to improved outcomes for mice infected with influenza, at risk of cancer metastasis, or genetically prone to lupus, its administration can lead to serosal inflammation and elevation of biomarkers of liver and kidney damage. Variants with reduced density of cationic charge through the interspersal of hydroxyl groups were evaluated as potentially better-tolerated alternatives. Notably, the variant PAMAM G3 50:50, similar in size as PAMAM G3 but with half the charge, was not toxic in cell culture, less associated with weight loss or serosal inflammation after parenteral administration, and remained effective in reducing glomerulonephritis in lupus-prone mice. Identification of such modified scavengers should facilitate their development as safe and effective anti-inflammatory agents.

INTRODUCTION

Inflammation is a crucial part of the immune response to injury and illness, but excessive or prolonged inflammation can drive disease by inducing tissue injury or perpetuating the inflammation to a pathologic extent. Nucleic acids and other cellular molecules released from dead or injured cells contribute to inflammatory signaling through interaction with pattern-recognition receptors (PRRs) by acting as damage-associated molecular patterns (DAMPs). PRRs for nucleic acids are usually on the inside of cells and include the toll-like receptors (TLRs). Activation of these receptors requires the uptake of DNA and RNA into cells, thus making extracellular nucleic acids a target for therapy. While necessary for host defense and injury response, DAMPs and related pathogen-associated molecular patterns (PAMPs) can also drive maladaptive immune responses and can lead to pathologic inflammation in allergy, malignancy, and autoimmune diseases like systemic lupus erythematosus (SLE).[1–3]

Anti-inflammatory therapies like non-steroidal anti-inflammatory drugs (NSAIDs) and corticosteroids can attenuate inflammation both acutely and chronically; glucocorticoids in particular can reduce morbidity and mortality of many diseases associated with persistent or excessive inflammation. However, over time these agents can cause immunosuppression as well as a host of complications such as diabetes and osteoporosis. In view of the side effects of NSAIDs and corticosteroids as well as their limited efficacy in many conditions, a need remains for therapies that act earlier in the damage-induced signaling cascade without causing immune suppression.

Dendritic polymers like poly(amidoamine) (PAMAM) have emerged as promising therapeutic candidates to mitigate such TLR-mediated inflammation.[4,5] Unlike specific TLR antagonists, such as the anti-TLR3 antibody PRV-300 and the TLR4 small molecule antagonist JKB121,[6] these highly branched, monodispersed, cationic molecules can bind and sequester a wide range of negatively charged cellular molecules, like RNAs, DNAs, and nucleic acid-containing complexes, away from their respective TLRs and

[1]Department of Surgery, Duke University, Durham, NC 27710, USA

[2]Department of Pharmacology and Cancer Biology, Duke University, Durham, NC 27710, USA

[3]Department of Chemistry, Duke University, Durham, NC 27710, USA

[4]Department of Medicine and Immunology, Division of Rheumatology, Duke University Medical Center, Durham, NC 27710, USA

[5]Department of Biology, Duke University, Durham, NC 27710, USA

[6]Collegiate School, New York, NY 10069, USA

[7]Department of Biomedical Engineering, Duke University, Durham, NC 27710, USA

[8]Medical Research Service, Veterans Administration Medical Center, Durham, NC 27705, USA

[9]Department of Pathology, Duke University, Durham, NC 27710, USA

[10]These authors contributed equally

[11]Lead contact

*Correspondence: bruce.sullenger@duke.edu

https://doi.org/10.1016/j.isci.2022.105542

other internal nucleic acid sensors. The binding and neutralization of nucleic acid-containing DAMPs/PAMPs by these molecules have been termed scavenging. As data from our laboratory has shown, treatment with PAMAM G3, the generation 3-sized dendrimer, displays beneficial anti-inflammatory effects in many murine models of disease and injury, including cutaneous lupus and lupus nephritis.[7–12] Mechanistically, PAMAM G3 is able to prevent the binding of DNA to anti-DNA antibodies, thereby blocking immune complex formation.[5,13] Immune complexes in SLE can deposit in the kidney and induce the production of pro-inflammatory cytokines such as type 1 interferon by cells of the innate immune system. Reducing the burden of immune complexes can thereby help slow the progression of lupus nephritis.[8]

Despite these promising findings in cell culture and *in vivo* models, therapeutic doses of PAMAM G3 can cause local and systemic toxicity in mice, limiting the nucleic acid scavenger's translational potential.[12] This toxicity increases with polymer generation due to the increased density of positive amine surface charges which double with each generation.[14,15] In contrast, the anionic and neutral surface group variants of PAMAM with carboxyl and hydroxyl surface end groups respectively are tolerated with minimal toxicity at much higher doses.[16–18] However, these molecules lack the charge profile to effectively bind and scavenge nucleic acid DAMPs.

We hypothesized that we could retain the scavenging properties of PAMAM and mitigate its toxicity by diluting the density of the positive surface charge of cationic PAMAM with neutral moieties. To investigate this possibility, we designed PAMAM generation 3 and 4 variants with a 50:50 mix of cationic and neutral surface groups and examined their scavenging function as well as their cellular and *in vivo* toxicity. Understanding the contribution of size and charge density to the scavenging function and toxicity profile of PAMAM will enable the rational design of biomaterials that retain anti-inflammatory properties but have less toxicity. The design of such agents will help realize the goal of safe and effective biomaterial-based therapy for lupus and other inflammatory diseases.

RESULTS

Mixed surface poly(amidoamine) polymers feature neutral hydroxyl groups that disperse the cationic moieties arrayed on their surface

The design of the mixed surface polymers, in comparison to PAMAM G3, is shown in Figure S1. The mixed polymer PAMAM G3 50:50 features 16 amine groups and 16 hydroxyl groups compared to the 32 amine groups on PAMAM G3's surface. The higher generation mixed polymer PAMAM G4 50:50 features 32 surface amine groups, as PAMAM G3 does, but they are interspersed with neutral hydroxy groups over a larger surface area. Other fully cationic PAMAMs besides PAMAM G3 were included for comparison in certain studies; these compounds include the smaller PAMAM G2 with 16 amine groups and the larger PAMAM G4 with 64 amine groups.

Mixed surface poly(amidoamine) variants scavenge nucleic acid-based toll-like receptor agonists

To justify further characterization, the mixed surface polymers should demonstrate a similar capacity for scavenging nucleic acid-based DAMPs/PAMPs as their fully cationic precursors. Therefore, the nucleic acid scavenging capacity of the mixed surface polymers was tested alongside the fully cationic PAMAMs. The prototypic DAMPs used were polyI:C, a synthetic analog of double-stranded RNA that mimics viral infection by stimulating TLR3, and CpG 1668, a modified DNA oligonucleotide containing an unmethylated CpG dinucleotide motif found enriched in bacterial genomes and mitochondrial DNA, that acts through TLR9. PAMAM G3 50:50 and G4 50:50 prevented TLR3 activation by polyI:C (Figure 1A) and TLR9 activation by CpG in a dose-responsive manner (Figure 1B) as well as or better than the fully cationic PAMAM variant with the same number of cationic end groups (e.g. compare PAMAM G3 50:50 to PAMAM G2). The concentrations at which the respective polymers inhibited TLR3 and TLR9 activation by 50% (IC50 values) are shown in panel D. For TLR3 signaling inhibition, for instance, about 7 times more G3 50:50, 15 times more G2, and similar amounts of G4 and G4 50:50 were required compared to the benchmark polymer G3. As expected, none of the cationic or mixed-surface polymers was able to prevent TLR4 activation by the non-nucleic acid agonist, lipopolysaccharide LPS-B5 except at extremely high concentrations, demonstrating the nucleic acid-DAMP/PAMP selectivity of the inhibition (Figure 1C).

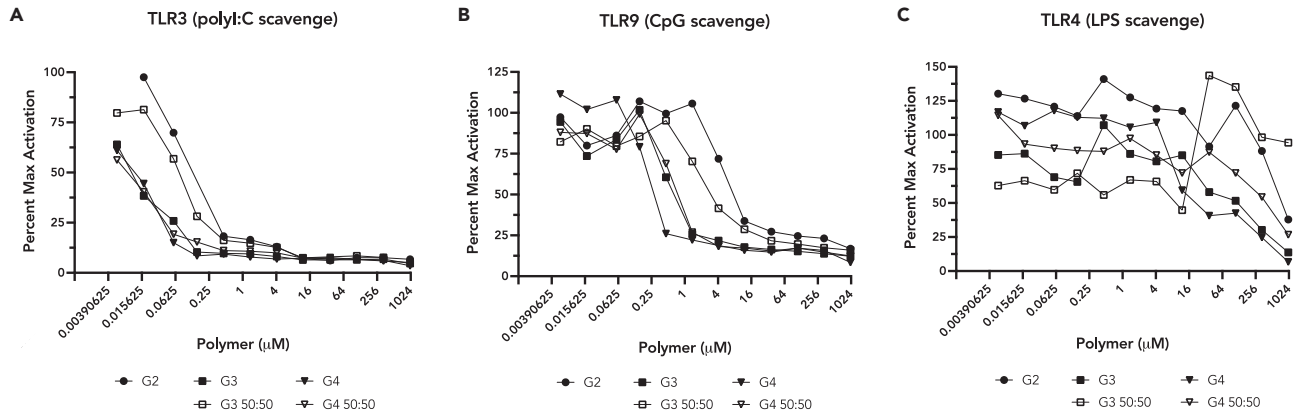

D

	G2 μm	G3 μm	G3 50:50 μM	G4 μM	G4 50:50 μM
TLR3 IC50	0.1524	0.0103	0.0697	0.0102	0.0064
TLR9 IC50	13.9300	0.8797	4.4200	0.3261	0.9225

Figure 1. Analysis of PAMAM variants for TLR inhibition

All PAMAM variants prevent the activation of TLR3 (A) and TLR9 (B) by effectively scavenging the nucleic acid agonists polyI:C and CpG, but do not effectively scavenge LPS, the canonical agonist of TLR4 (C)

Each point is the mean of three replicates. Calculated IC50 values for the inhibition of TLR3 and TLR9 signaling by the polymers (D).

Poly(amidoamine) G3 and mixed surface poly(amidoamine) variants bind nucleic acids with similar thermodynamic parameters

Isothermal Titration Calorimetry (ITC) was employed to assess the nucleic acid binding thermodynamics and stoichiometry of the PAMAM polymers bearing different surface cation numbers and densities. Specifically, PAMAM G3, G3 50:50, and G4 50:50 dendrimers were titrated into a solution of CpG 1668 oligonucleotide in PBS, and a separate titration of each polymer to PBS was used to correct the dissolution heat. The raw heat data, corrected for dilution and integrated, yielded thermograms with a biphasic pattern suggestive of a two-site binding mechanism between PAMAM and CpG (Figure S2). The thermograms were therefore fitted using an independent two-site binding model. The best-fit values for the associated thermodynamic parameters are shown in Table 1. The result showed that all polymers have similar binding stoichiometries and binding mechanisms; the first set of binding sites can bind 2-3 CpGs per polymer. This

Table 1. Thermodynamic parameters of first-site binding and second-site binding between each polymer and the CpG 1668 oligonucleotide

First Site	n1	Kd1	ΔH1 (kJ/mol)	ΔS1 (J/mol·K)	CpG/Polymer
PAMAM G3	0.449	4.32E-9	−428	−1280	2.23
PAMAM G3 50:50	0.340	1.68E-7	−149	−371	2.94
PAMAM G4 50:50	0.411	4.602E-8	−444	−1350	2.43
Second Site	**n2**	**Kd2**	**ΔH2**	**ΔS2**	**CpG/Polymer**
PAMAM G3	0.100	3.39E-7	742	2610	≥10
PAMAM G3 50:50	0.100	4.07E-6	436	1570	≥10
PAMAM G4 50:50	0.100	1.66E-6	1070	3710	≥10

n: stoichiometric ratio of polymer to the CpG oligonucleotide.

Kd (M): dissociation constant.

ΔH (kJ/mol): enthalpy change.

ΔS (J/mol·K): entropy change.

For each polymer, isothermal titration calorimetry results were corrected for the heat of dilution and the integrated heat data were fitted with a two-site binding model in the program Nano Analyze. The best-fit parameters resulting from the nonlinear regression fit of the data are shown. See also Figure S2.

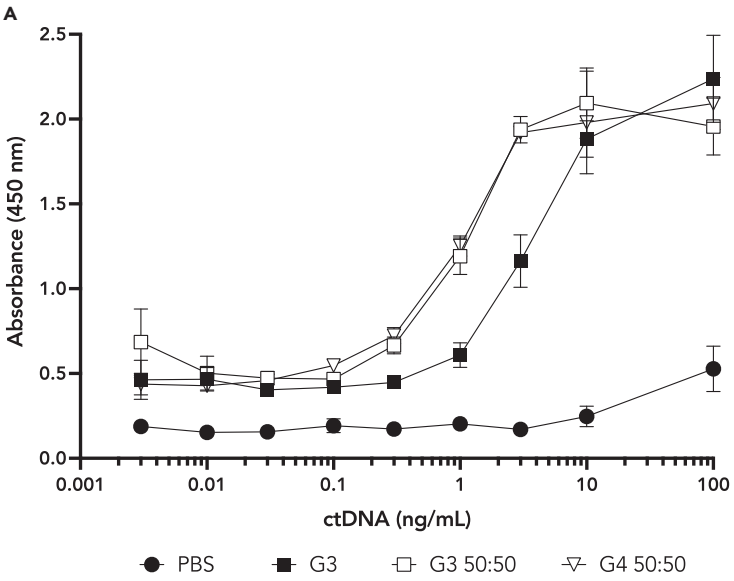

B

ctDNA [ ]	Summary	Adjusted P Value
0.3 ng/mL		
G3 vs G3 50:50	ns	0.4930
G3 vs G4 50:50	ns	0.2827
G3 50:50 vs G4 50:50	ns	0.9817
1 ng/mL		
G3 vs G3 50:50	**	0.0014
G3 vs G4 50:50	***	0.0003
G3 50:50 vs G4 50:50	ns	0.9803
3 ng/mL		
G3 vs G3 50:50	****	<0.0001
G3 vs G4 50:50	****	<0.0001
G3 50:50 vs G4 50:50	ns	0.9996
10 ng/mL		
G3 vs G3 50:50	ns	0.5201
G3 vs G4 50:50	ns	0.9206
G3 50:50 vs G4 50:50	ns	0.8824

Figure 2. Mixed surface PAMAM variants capture double-stranded ctDNA (calf thymus DNA) at least as, if not more, effectively than the fully cationic PAMAM G3 molecule in "sandwich-type" ELISA assays

(A) Plot of binding of ctDNA with data shown as mean ± standard error of the mean.

(B) A two-way ANOVA with post hoc analysis via Tukey's multiple comparison test demonstrates that the mixed polymers bind ctDNA more efficiently than G3 at 1 ng/mL and 3 ng/mL ctDNA concentrations.

ratio is expected because the 16-32 amine groups on each polymer can simultaneously interact with negatively charged phosphate groups on different CpG molecules. The binding stoichiometry is not a whole number, possibly related to a non-specific binding mechanism wherein the capacity of each polymer molecule cannot be well-defined. As expected, this interaction between polymers and CpG is enthalpy favored ($\Delta H < 0$) due to the electrostatic interaction formed during binding. At the same time, entropy is unfavored due to the limitation of free movements of the molecules upon binding. Interestingly, despite different sizes, cation numbers, and cation densities, the three polymers did not significantly differ in CpG binding capacity. On the other hand, the dissociation constants varied over a forty-fold range. PAMAM G3, with a higher cation density, demonstrated the highest binding affinity for the DNA oligonucleotide (K_D = 4.32 nM), while PAMAM G3 50:50 possessing both lower cation number and density showed the lowest binding affinity (K_D = 168 nM). Nonetheless, all three polymers have nanomolar affinities to the CpG oligonucleotide which is consistent with their common ability to scavenge DNA and RNA (Figure 1). The second set of binding sites for each polymer showed an unrealistically high binding capacity ($\geq$10 CpG per polymer) and is unexpectedly entropy-driven. We surmise that this binding process represents the non-specific adsorption of CpG to impurities in the polymer preparation or the formation of higher order complexes. Elimination of such impurities or complex formation at high concentrations is difficult to accomplish due to the heterogeneous nature of polymer synthesis and spontaneous aggregation of the polymers in storage. We, therefore, omit further analysis of this binding site.

Mixed surface poly(amidoamine) variants bind native double-stranded DNA and inhibit the recognition of that DNA by an anti-DNA antibody

PAMAM G3 has been shown to bind DNA and inhibit the binding of anti-DNA antibodies, which is likely a factor in its effects in lupus-prone animals.[8,13] The mixed surface variants were compared to PAMAM G3 in enzyme-linked immunosorbent assays (ELISAs) that assessed the capture of double-stranded calf thymus DNA (ctDNA) and the inhibition of anti-DNA antibody binding to ctDNA. In the ELISA shown in Figure 2, equal amounts by weight of each polymer (100 ng: 14.5 pmol G3, 14.4 pmol G3 50:50, and 7.0 pmol G4 50:50) were used to coat each well, a dilution series of ctDNA was applied, followed by washing and detection of captured ctDNA using the anti-DNA antibody Val-1205. The mixed surface polymers generated a dose-responsive signal with ctDNA concentrations at 0.3 ng/mL and greater while the fully cationic G3 required at least 1 ng/mL ctDNA for signal and was consistently less efficient in capturing DNA than the G3 50:50 variant. Selected results from a two-way ANOVA analysis shown in panel B reveal that between

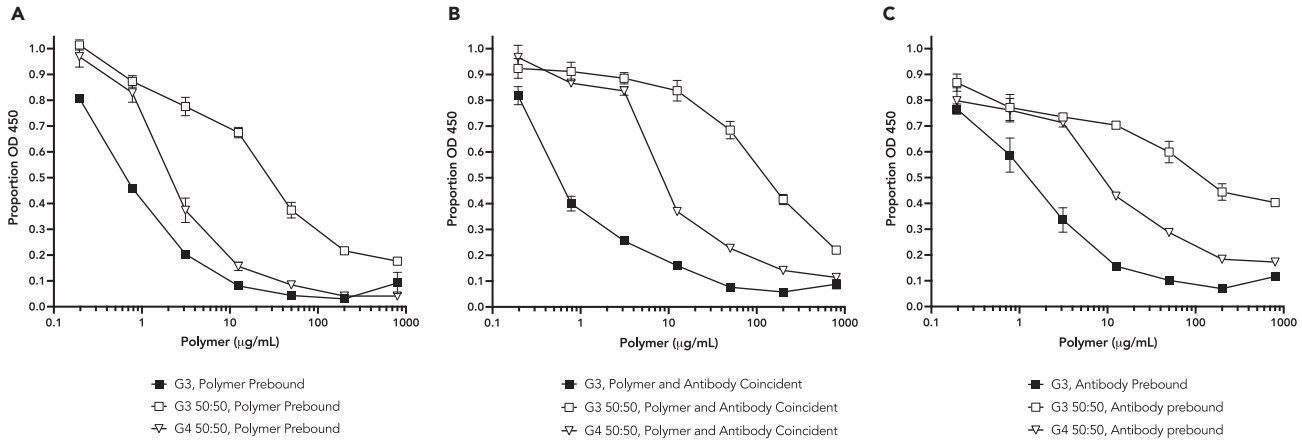

D

	G3 μg/mL	G3 50:50 μg/mL	G4 50:50 μg/mL
Polymer prebound IC50	0.74	29.24	2.41
Coincident IC50	0.77	129.20	10.83
Antibody prebound IC50	1.24	153.80	9.69

Figure 3. PAMAM G3 and mixed surface variants G3 50:50 and G4 50:50 inhibit anti-DNA antibody binding to DNA in competition ELISAs

(A) Blocking of antibody binding.

(B) Competition with antibody binding.

(C) Displacement of antibody binding. For panels A, B, and C, data are mean ± standard error of the mean.

(D) Calculated IC50 values for the inhibition of antibody binding by the polymers.

the baseline signal and peak signal, the mixed polymers bind and capture DNA significantly better than parental PAMAM G3 in this ELISA format.

Mixed surface PAMAM variants were then assessed in comparison to PAMAM G3 for their effects on the interaction between DNA and the monoclonal anti-DNA Val-1205 antibody. A uniform amount of ctDNA (100 ng) was allowed to bind to each well. Polymers were then added either prior to the antibody (Figure 3A), together with the antibody (Figure 3B), or after the antibody (Figure 3C). The concentrations at which the respective polymers interfered with antibody binding to DNA by 50% (IC50 values) are shown in panel D. Relatively low concentrations of PAMAM G3 were capable of limiting the association of the antibody with DNA, with 50% antibody binding inhibition occurring with polymer concentrations on the order of 1 μg/mL. In addition, the blocking did not appear sensitive to the relative order of addition of the polymer and the antibody. About 10-fold more of the larger polymer, G4 50:50 was needed for the similar inhibition of antibody binding, with less needed if the polymer was added prior to antibody addition. Notably, G3 50:50, with half the overall cationic charge of PAMAM G3, required a 100-fold greater concentration than PAMAM-G3 to disrupt antibody-DNA binding and was less effective in competing against prior to binding of the antibody (Figure 3C). The reduced ability of G3 50:50 to compete anti-DNA antibody to DNA binding is consistent with our ITC results (Figure 1).

Mixed surface poly(amidoamine) variants show significantly reduced cytotoxicity compared to the fully cationic forms

The mixed surface PAMAM variants with more diffuse surface charge were compared to the fully cationic forms for effects on cell viability in culture. HEK293 cells were exposed to the PAMAM variants for 24 h and relative cytotoxicity was assessed by comparing ATP levels using CellTiter-Glo®. Fully cationic PAMAMs G2, G3, and G4 reduced cell viability, with toxicity increasing by generation as previously reported.[15] In contrast, PAMAM G3 50:50 with half its 32 end groups replaced with hydroxyl groups caused no cytotoxicity even at concentrations exceeding 1 mM, while PAMAM G4 50:50, which shares molecular size with G4 but has half of its 64 end groups replaced with hydroxyl groups, caused no cytotoxicity to concentrations of 333 μM and was still less cytotoxic than PAMAM G2 at the highest dose tested (Figure 4).

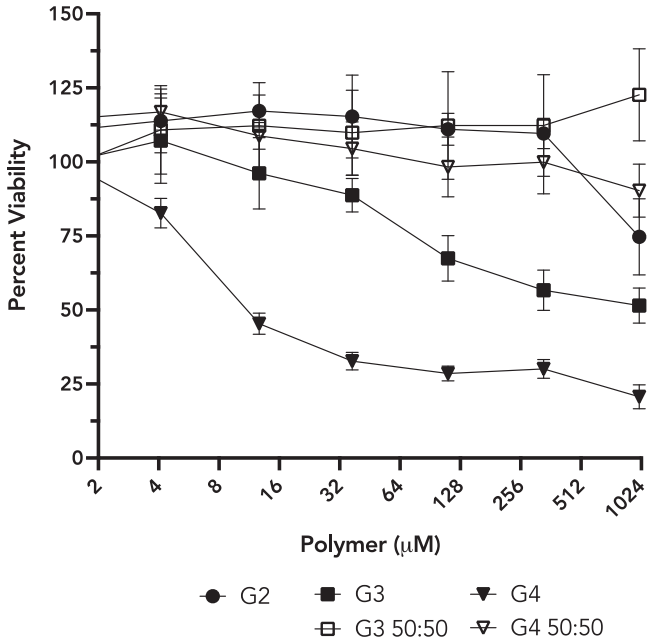

	Summary	Adjusted P Value
1000 μM		
G3 50:50 vs. G3	****	<0.0001
G4 50:50 vs. G4	****	<0.0001
333 μM		
G3 50:50 vs. G3	**	0.0015
G4 50:50 vs. G4	****	<0.0001
111 μM		
G3 50:50 vs. G3	*	0.0188
G4 50:50 vs. G4	****	<0.0001

Figure 4. When assessed after 24-h treatment of HEK293 cells, mixed surface PAMAM variants have reduced toxicity compared to fully cationic PAMAMs

(Left) Plot of percent viability with data shown as mean with ± standard error of the mean.

(Right) A two-way mixed ANOVA with post hoc analysis via Tukey's multiple comparison test demonstrates that the mixed polymers are significantly less toxic than their same sizes fully cationic polymers at several matched concentrations. Selected comparisons are shown.

Considering that DAMP signaling is particularly prominent in immune cells and the scavenger benefits likely arise from sustained inhibition of inflammatory signaling, assessment of nucleic acid scavenger effects on the viability of an immune cell line over time is informative. We assessed toxicity using the murine macrophage cell line RAW 264.7. As shown in Figure 5, from 24 h (panel A), to 48 h (panel B), to 72 h (panel C), PAMAM G3 manifested toxicity at much lower concentrations than G3 50:50. Results from two-way mixed ANOVAs with post hoc analysis via Sidak's multiple comparison tests reveal that G3 50:50 was significantly less toxic than G3 over a wide concentration range. Even after 72 h, at the highest concentration tested, essentially no cells treated with G3 were viable while 50% of G3 50:50 treated cells remained viable.

Mixed surface poly(amidoamine) variants circumvent *in vivo* toxicity of cationic poly(amidoamine)

Given the reduced toxicity associated with mixed surface polymers in cell culture, we next examined whether the mixed polymers would be better tolerated *in vivo*. In three short-term toxicity studies, 20 mg/kg (low dose) and 40 mg/kg (high dose) doses of polymer were delivered to young female C57BL/6J mice. The mice were dosed intraperitoneally every third day for four total doses (days 0, 3, 6, and 9) and sacrificed on day 10. To assess if any polymer effects were transient, an additional set of mice were treated at 40 mg/kg with the same dosing regimen as above, with half sacrificed on day 10 as part of one of the short-term toxicity cohorts and the remaining mice left for an additional 14 days with no further treatment, sacrificed at day 24, and designated as the recovery cohort. The 20 mg/kg and 40 mg/kg doses were chosen as we previously determined that the maximum tolerated dose of PAMAM G3 is 100-200 mg/kg and the 20 mg/kg dose was found to be therapeutic in lupus prone animals (Holl, Shumansky et al. 2016).

The fully cationic and mixed surface variants were first compared for their effects on mouse body weight. For all mice, weight was measured daily for the first 10 days (Figure 6) and then for those mice in the recovery cohort every two days from day 10 to day 24 (Figure S3). The only exception to the planned regimen was the PAMAM G4 40 mg/kg group that was sacrificed 24 h after the first dose due to acute toxicity. A mixed-effects analysis of weight in the low-dose treatment groups (20 mg/kg) was performed to determine the effect of polymer treatment over time. Polymer treatment had a significant effect on weight ($p = 0.0002$).

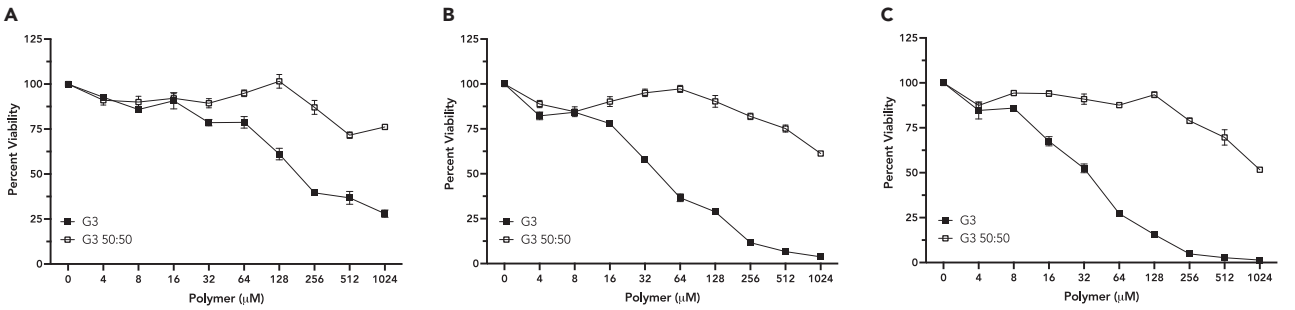

24 hours
Šídák's Multiple Comparisons Test

	Summary	Adjusted P Value
G3 - G3 50:50		
0	ns	>0.9999
4	ns	>0.9999
8	ns	0.956
16	ns	>0.9999
32	ns	0.0518
64	***	0.0008
128	****	<0.0001
256	****	<0.0001
512	****	<0.0001
1024	****	<0.0001

48 hours
Šídák's Multiple Comparisons Test

	Summary	Adjusted P Value
G3 - G3 50:50		
0	ns	>0.9999
4	ns	0.125
8	ns	>0.9999
16	***	0.0002
32	****	<0.0001
64	****	<0.0001
128	****	<0.0001
256	****	<0.0001
512	****	<0.0001
1024	****	<0.0001

72 hours
Šídák's Multiple Comparisons Test

	Summary	Adjusted P Value
G3 - G3 50:50		
0	ns	>0.9999
4	ns	0.9769
8	*	0.0392
16	****	<0.0001
32	****	<0.0001
64	****	<0.0001
128	****	<0.0001
256	****	<0.0001
512	****	<0.0001
1024	****	<0.0001

Figure 5. When assessed after a treatment time course of mouse macrophage RAW 264.7 cells, the mixed surface PAMAM variant G3 50:50 has significantly reduced toxicity compared to fully cationic G3

Cells were exposed for 24 h (A), 48 h (B), and 72 h (C). Data in graphs are mean ± standard error of the mean. Below each graph results from a two-way mixed ANOVA with post hoc analysis via Sidak's multiple comparison test identifying the concentrations at which there is a significant difference between G3 and G3 50:50 treatments.

Posthoc comparison of polymer treatment to saline showed significant weight loss on several days for G2 (days 1, 6, 9, and 10), G3 (days 1, 2, 4, and 7) and G4 (days 1-4, 7, 8, and 10) treated mice. As well, PAMAM G3 and G4-treated mice exhibited a telling pattern with an obvious weight dip the day after each dosing and recovery through the next two days. In contrast, the mixed surface polymer-treated mice showed no patterned response to dosing and there was a very rarely difference in weight between them and saline-treated mice (day 1 for G3 50:50 and day 9 for G4 50:50) (Figure 6A).

In the high dose group (40 mg/kg, Figure 6B) polymer was found to have a significant impact on weight in mixed-effects analysis ($p < 0.0001$). In posthoc evaluation, G2 and G3 treated mice weighed less than the saline-treated mice at all timepoints following treatment on day 0. G4-treated mice also weighed significantly less than the saline-treated mice on day 1 but were excluded from the repeated measures analysis because of the acute toxicity which required sacrifice on day 1. G3 50:50 treated animals also weighed significantly less than the saline-treated mice on all days but day 1, but the mean difference throughout was smaller than that for the fully cationic polymers at all timepoints, as demonstrated for day 10 (Figure 6C). G4 50:50 treatment was the mildest in terms of weight loss compared to saline. Cessation of treatment for 14 days prior to sacrifice ameliorated weight loss in mice that had been treated with the PAMAM G2 and G3 at 40 mg/kg (Figure S3). During this period, the mice in the recovery cohort that had been treated with the mixed surface polymers maintained a relatively stable body weight, while the mice that had been treated with cationic polymers G2 and G3 dramatically rebounded in weight, catching up to the other treatment groups. Thus, the PAMAM G3 50:50 and G4 50:50 variants demonstrate a much reduced negative impact on animal weight compared to fully cationic PAMAM polymers.

At time of sacrifice for the short-term toxicity experiments, (day 10 for all mice save for G4 at 40 mg/kg, which were sacrificed on day 1 due to acute toxicity), whole blood was collected for complete blood count and serum chemistry analysis, and organs were weighed and fixed. Liver and kidney function tests were performed using mouse serum (Figure 7). Mice treated with the single 40 mg/kg dose of PAMAM G4 had marked elevations in AST and ALT, indicative of acute liver toxicity. All mice treated with the fully cationic PAMAMs at 40 mg/kg had mild elevations in both BUN and creatinine, indicative of kidney injury. By contrast, treatment with the PAMAM 50:50 variants, even at the higher dose, did not result in the notable elevation in any of these liver and kidney toxicity markers. Complete blood count revealed relative

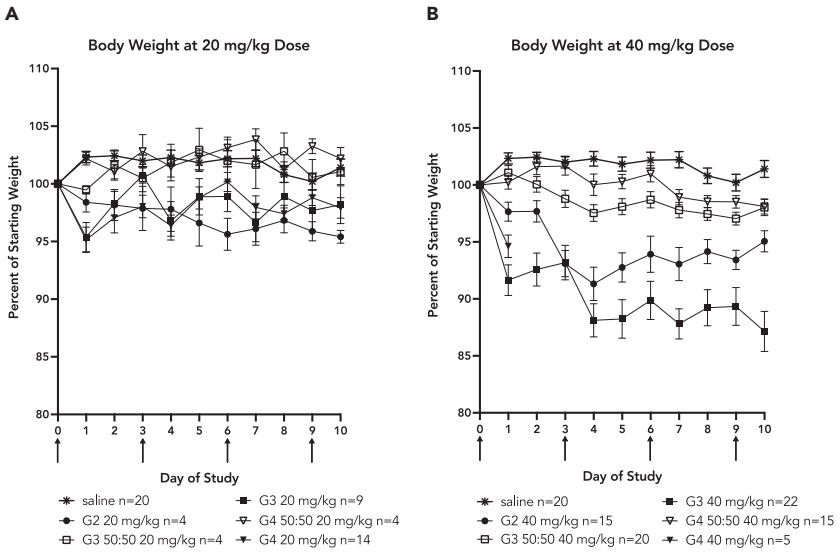

C

Dunnett's Multiple Comparisons Test	Mean Difference	Summary	Adjusted P Value
Day 10 40 mg/kg			
Saline vs. G2	6.347	****	<0.0001
Saline vs. G3 50:50	3.389	**	0.0078
Saline vs. G3	14.26	****	<0.0001
Saline vs. G4 50:50	3.289	**	0.0085

Figure 6. Mixed surface scavengers are associated with reduced weight loss compared to treatment with fully cationic scavengers

Scavengers were administered to C57BL/6J mice by intraperitoneal injection on days 0, 3, 6, and 9. Mixed-effects analysis of normalized body weights followed by post hoc analysis via Dunnett's multiple comparisons test identified fewer significant differences at the 20 mg/kg dosing than at the 40 mg/kg dosing. Data in graphs are mean ± standard error of the mean.

(A) Body weight of mice dosed at 20 mg/kg.

(B) Body weight of mice dosed at 40 mg/kg. Mice treated with G4 at 40 mg/kg were sacrificed 24 h after the first dose due to drug toxicity.

(C) Table comparing each scavenger treatment (dosed at 40 mg/kg) to saline treatment on day 10. See also Figure S3.

lymphopenia (Figure 8A) and granulocytosis (Figure 8B) in mice treated with 40 mg/kg of cationic PAMAM G2, G3, and G4, suggesting an acute inflammatory response to treatment with these dendrimers; notably, these effects were much milder in the mice that had been dosed at 20 mg/kg. By contrast, no significant change in lymphocytes and granulocytes was observed in the mixed dendrimers-treated animals. Further evaluation of the inflammatory consequences of PAMAM G3 led us to assess serum levels of inflammatory cytokines using multi-analyte flow cytometry. As shown in Figure 8C, the cytokine IP-10 (CXCL10) was significantly elevated in G3 40 mg/kg treated mice relative to saline-treated and G3 50:50 treated mice. IP-10 is a proinflammatory chemokine that causes the migration of leukocytes, including monocytes, NK cells, T-cells, and dendritic cells.[19] Cytokine IL-6, which broadly stimulates inflammatory and autoimmune processes, and cytokine CXCL1 (KC), a potent neutrophil attractant, also trended higher in the G3 40 mg/kg treated mice; in G3 50:50 40 mg/kg mice they were appreciably lower, with amounts closer to those of saline mice. These cytokine results indicate that the mixed surface polymer G3 50:50 is less proinflammatory than G3 at 40 mg/kg.

Histologic analysis reveals that serosal inflammation is triggered by the fully cationic polymer G3 and reduced in mice treated with mixed surface polymers

While there were no obvious differences between groups on necropsy or differences in organ weights (data not shown), we carried out the histological analysis of the liver, diaphragm, and kidneys of mice from G3, G3 50:50, and G4 50:50 treatment groups. Serosal inflammatory changes in mice treated intraperitoneally with fully cationic PAMAM G3 at 20 mg/kg and 40 mg/kg were evident in histological analysis. While PAMAM G3 treated mice exhibited the inflammation of the liver capsule, no mice treated with PAMAM G3 50:50 and only two of the nine mice treated with PAMAM G4 50:50 at 40 mg/kg demonstrated this liver surface inflammation consisting of a pleocellular infiltration of neutrophils, macrophages, and lymphoid cells (Figure 9A and compare Panels B-E). Notably, for the PAMAM G3 recovery cohort, the effect was sustained even following the two-week recovery period. Liver capsule inflammation was still significant in mice dosed at 20 mg/kg PAMAM G3, in keeping with earlier findings,[12] and shown in Figure S4. Most obvious on the liver, this capsular inflammation is likely a compound surface property effect from direct contact of the material with cells during the intraperitoneal administration of the compound. Basophilic globules presumed to be dendrimer compound were noted in association with the cellular infiltrate. Other than the surface changes

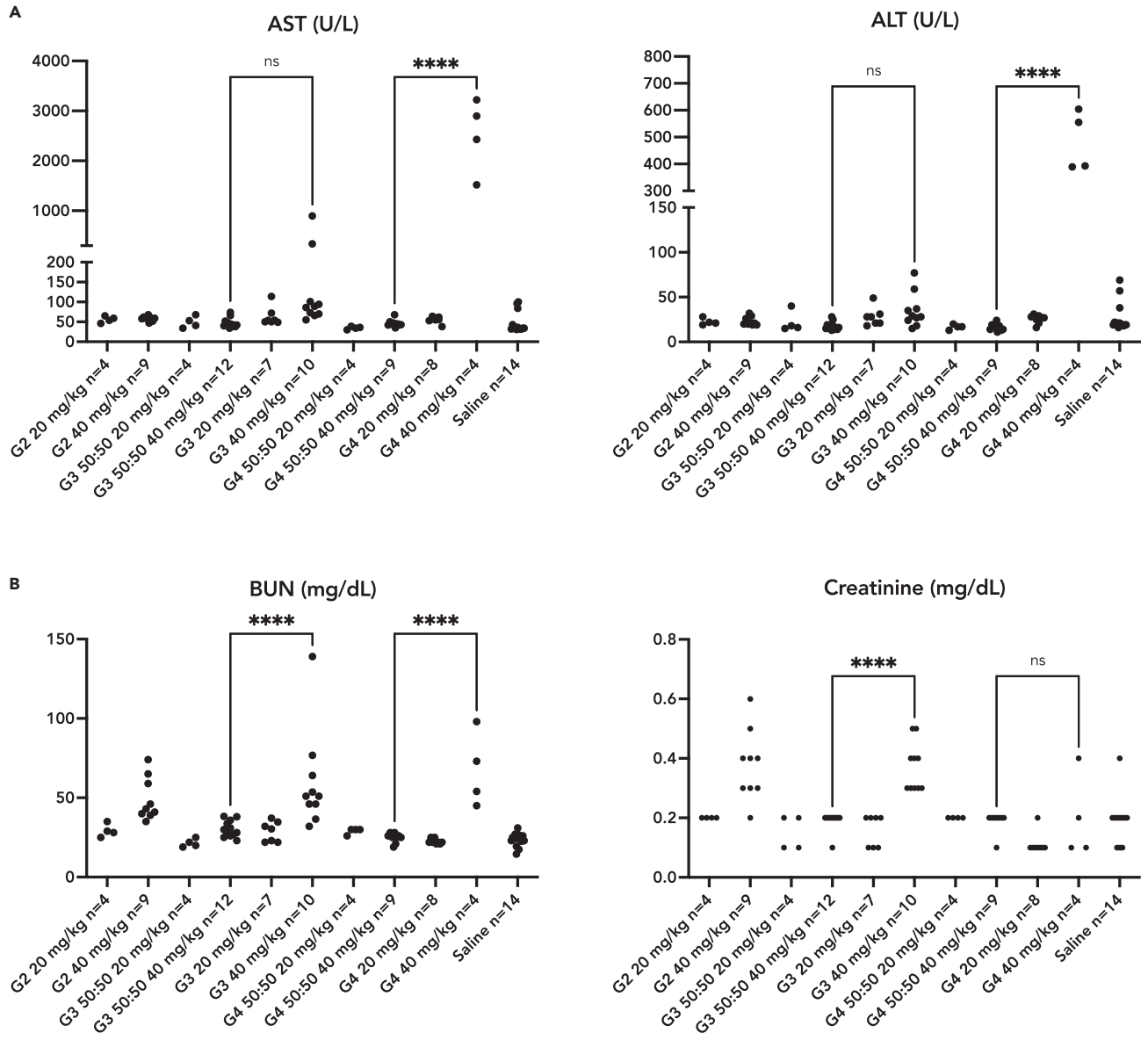

Figure 7. Serum liver and kidney function tests indicate liver and kidney injury when treating with fully cationic PAMAM polymers

Scavengers were administered to C57BL/6J mice by intraperitoneal injection on days 0, 3, 6, and 9, with sacrifice on day 10 with blood collection for serum.

(A) Elevated AST (aspartate aminotransferase) and ALT (alanine transaminase) suggest liver injury at 40 mg/kg dose of PAMAM G4.

(B) Elevated BUN (blood urea nitrogen) and creatinine indicate kidney injury with the fully cationic PAMAMs at 40 mg/kg. No such injury is seen after treatment with the mixed surface scavenger variants.

Ordinary one-way ANOVAs followed by Tukey's multiple comparisons tests were run for each of the markers; comparisons between generation-matched fully cationic and mixed surface scavengers are specified. Significance: ****represents $p < 0.0001$.

described above, no histologic signs of hepatocytic toxicity were observed in the deeper hepatic parenchyma.

Fortuitous sampling followed by the direct study of additional peritoneal organs revealed widespread inflammation of other serosal surfaces upon treatment with PAMAM G3 at 40 mg/kg. The mice treated with fully cationic G3 exhibited severe inflammation of the diaphragm surface and muscle particularly on the abdominal side (Figure 10) and inflammation of the pancreatic interstitial tissue and peripancreatic fat (data not shown). The diaphragm inflammation seen in G3-treated mice was persistent, with no apparent alleviation in the recovery cohort. The diaphragm surface inflammation presumably is a similar

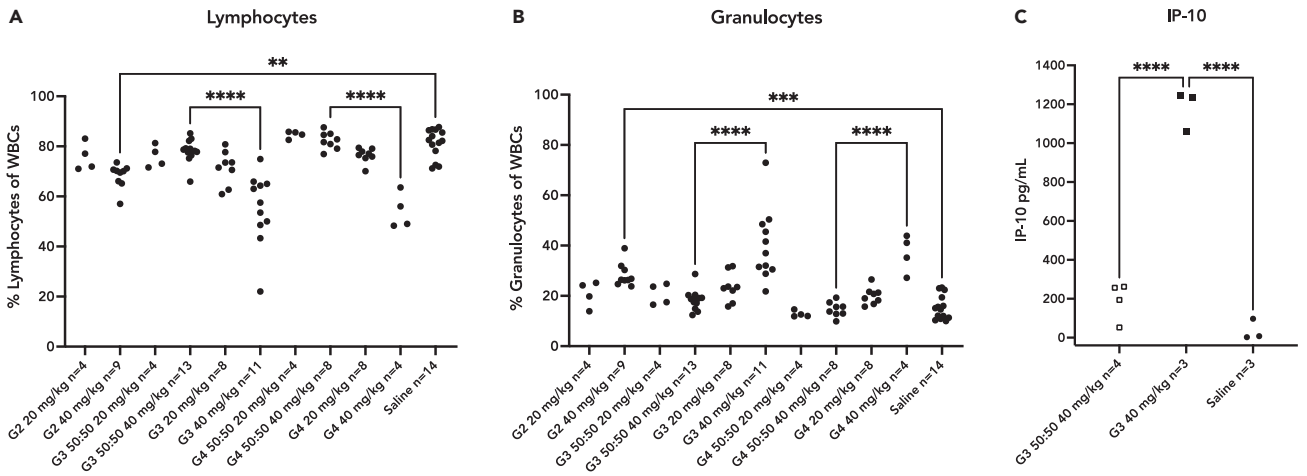

Figure 8. Fully cationic PAMAMs at 40 mg/kg elicit an acute inflammatory response

This acute inflammatory response to treatment with fully cationic PAMAMs at 40 mg/kg is demonstrated by decreased lymphocyte percentage (A) and increased granulocyte percentage (B) in blood, and elevation of the inflammatory cytokine IP-10 (C) in serum. No such response is seen with mixed surface scavenger treatments. Scavengers were administered to C57BL/6J mice by intraperitoneal injection on days 0, 3, 6, and 9, with sacrifice on day 10 with blood collection for complete blood counts and for serum.

Ordinary one-way ANOVAs followed by Tukey's multiple comparisons tests were run for each of the markers; for panels A and B, comparisons between generation-matched fully cationic and mixed surface scavengers, and between G2 40 mg/kg to saline, are specified. Significance: ** represents $p = 0.0017$, *** represents $p = 0.0009$ and **** represents $p \leq 0.0001$.

direct contact-induced effect from where the compound exits through the diaphragmatic lymphatics following IP injection (data not shown). Very mild inflammation of the diaphragm was seen acutely in some of the G3 50:50 mice at 10 days and was not seen at all in the G3 50:50 recovery cohort at 24 days. Mice treated with G4 50:50 exhibited moderate inflammation of the diaphragm, and occasional inflammation of the pancreas and associated fat as well, evident in both short-term and recovery cohort mice. Overall, compared to fully cationic PAMAM G3, there was reduced inflammation with G4 50:50 treatment and almost none with G3 50:50 treatment.

Poly(amidoamine) treatment induces kidney lesions

Renal cortical tubular changes were noted in all PAMAM-treated mice, whether treated with fully cationic PAMAM G3 or either of the mixed surface variants. Eosinophilic protein droplet accumulations and nephropathic changes (tubular basophilia and regeneration with hypertrophy and hyperplasia) were observed in treated animals and both tubular lesions were graded semi-quantitatively on a 0-4 scale, with 0 indicating normal kidney and 4 indicating marked change, as described in the STAR Methods. The quantitation of these lesions is shown in Figure 11 and examples of these lesions are shown for all the dendrimer treatment groups in Figures 12 and 13. All three PAMAM variants elicit these changes with similar severity in contrast to their disparate effects on kidney function tests. Of note, for all three polymers, the protein droplet accumulation (Figure S5A) and the nephropathy (Figure S5B) were significantly less severe in mice dosed at 20 mg/kg. Protein droplets significantly diminished after the cessation of dosing with G3 50:50 and G4 50:50 for two weeks (Figure S6A). As well, nephropathy scores trended downward for all three polymers with recovery (Figure S6B). Of note, small 1 to 5 micron basophilic droplets, believed to be dendrimer compound, are present in all renal sections with lesions graded moderate or greater. Thus, though the inflammatory effects elicited by the fully cationic polymer were reduced when using the mixed PAMAM variants (Figures 9, 10, and S4), the renal depositions characteristic of PAMAM G3 use were not. However, it is unclear what the phenotype if any these alterations may cause given that the mixed polymer treatments did not result in the elevation of kidney damage markers (Figure 7B).

Long-term poly(amidoamine) G3 50:50 treatment reduces glomerulonephritis in lupus-prone MRL-lpr mice

Following the demonstration of the *in vitro* scavenging competency and overall reduced toxicity in cells and mice, we next assessed if the mixed surface PAMAM variants retained functionality in a mouse model of inflammatory disease. Our group has previously shown that 10 weeks of PAMAM G3 treatment (20 mg/kg

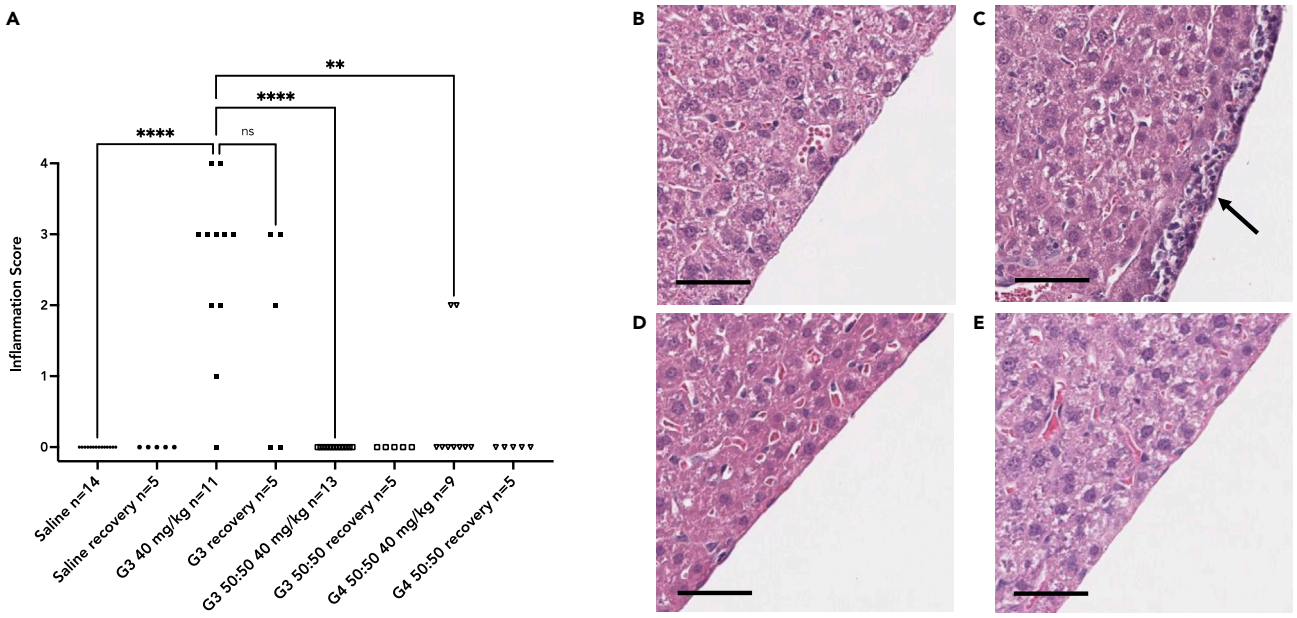

Figure 9. Short-term treatment with fully cationic PAMAM G3 at 40 mg/kg leads to persistent liver inflammation that is substantially less upon treatment with the mixed surface scavengers

(A) Histological scoring for liver inflammation in C57BL/6 mice upon treatment with four doses of indicated polymer at 40 mg/kg and sacrifice on day 10 or at day 24 after 14 days of recovery. Treatments were compared using the Kruskal-Wallis test followed by post hoc analysis via Dunn's multiple comparisons test. Significance: ** represents $p = 0.0032$ and **** represents $p \leq 0.0001$.

(B) Liver of saline-treated mouse.

(C) Liver of G3-treated mouse (40 mg/kg) with capsular inflammation (arrow).

(D) Liver of G3 50:50-treated mouse (40 mg/kg).

(E) Liver of G4 50:50-treated mouse (40 mg/kg).

Bar indicates 50 μM. See also Figure S4.

twice weekly) beginning at 10 weeks of age reduces glomerulonephritis in MRL-*lpr* male mice.[8] The MRL-*lpr* strain is a model of systemic lupus erythematosus; the mice have a genetic defect in Fas-mediated apoptosis of auto-reactive B and T cells, resulting in high levels of anti-DNA antibodies and spontaneous development of complex-mediated nephritis by 6 months of age. To assess the *in vivo* DAMP scavenging ability of mixed surface PAMAM variants, female and male MRL-*lpr* mice were treated twice weekly with 20 mg/kg PAMAM G3, 40 mg/kg G3 50:50, 40 mg/kg G4 50:50, or saline for 9 or 10 weeks beginning at 9 or 10 weeks of age respectively. Higher dosages of the 50:50 molecules were used to match total cationic end groups (G3 50:50) or number of molecules (G4 50:50) with 20 mg/kg cationic G3 treatment. Female mice began treatment and were sacrificed earlier because of the faster progression of lupus-like manifestations in this sex. At 18 or 20 weeks of age, mice were sacrificed and kidneys assessed for the severity of glomerulonephritis.

MRL-*lpr* mice develop membranoproliferative glomerulonephritis, characterized by glomerular hypercellularity and thickening of the glomerular basement membrane. Lymphoproliferative changes and tubular changes were not scored as part of the lupus assessment. Glomerular change was scored from 0 (normal), 1 (minimal), 2 (mild), 3 (moderate), through 4 (severe), and results are displayed in Figure 14 (females Panel A, males Panel B). Application of Kruskal-Wallis non parametric tests revealed that both the female treatment group medians varied significantly (p value = 0.0033) and the male treatment group medians varied significantly (p value = 0.0101). Post hoc evaluation via Dunn's multiple comparisons test involved the comparison of each polymer to the saline control, to evaluate whether any polymer mitigates the disease evident in the saline-treated mice. In female mice, PAMAM G3 50:50 treatment significantly improved glomerular scores compared to saline treatment (for G3 50:50 adjusted p value 0.0014) while treatment with PAMAM G3 just reached significance (for G3 adjusted p value 0.0441). Similarly in male mice, PAMAM G3 50:50 and PAMAM G3 each improved glomerular scores over saline treatment (for G3 50:50 adjusted p value 0.0100 and for G3 adjusted p value 0.0376). In contrast, the higher generation PAMAM

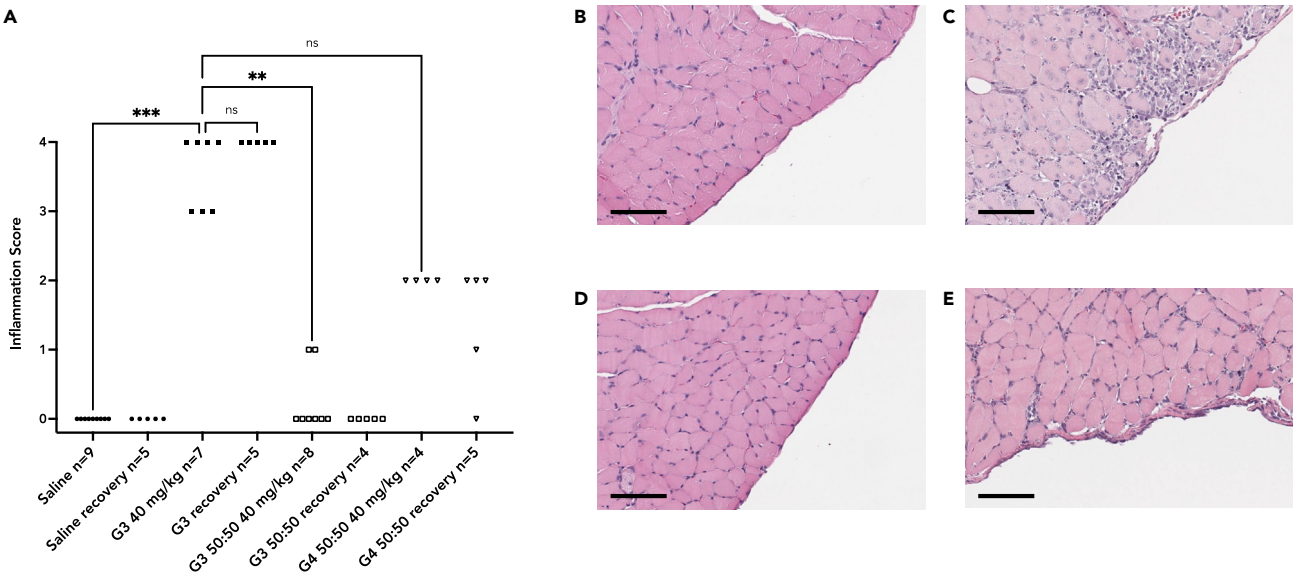

Figure 10. Short-term treatment with fully cationic PAMAM G3 at 40 mg/kg leads to persistent inflammation of the diaphragm surface and muscle that is less severe upon treatment with the mixed surface scavengers

(A) Histological scoring for the inflammation of the diaphragm in C57BL/6 mice after treatment with four doses of indicated scavenger at 40 mg/kg, with sacrifice on day 10 or at day 24 after 14 days of recovery. Treatments were compared using the Kruskal-Wallis test followed by post hoc analysis via Dunn's multiple comparisons test. Significance: ** represents p = 0.0066, *** represents p = 0.0004.

(B) Diaphragm of saline-treated mouse.

(C) Diaphragm of G3-treated mouse (40 mg/kg).

(D) Diaphragm of G3 50:50-treated mouse (40 mg/kg).

(E) Diaphragm of G4 50:50-treated mouse (40 mg/kg).

Bar indicates 100 μM.

G4 50:50 polymer failed to alleviate glomerulonephritis. Histological preparations of glomeruli of female MRL-*lpr* mice treated with saline, G3, G3 50:50, and G4 50:50 are shown in Figure 15.

DISCUSSION

In this study, we performed experiments to explore whether the toxicity associated with the cationic PAMAM G3 can be reduced while retaining the nucleic-acid scavenging functionality that underpins its anti-inflammatory pharmacologic effects. Specifically, we designed and tested two mixed-surface PAMAM variants, PAMAM G3 50:50 and G4 50:50, which each have molecular weight near that of their corresponding fully cationic PAMAM of the same generation but have half of their cationic amine end groups replaced with neutral hydroxyl groups. Our results indicate that these mixed surface polymers retain the nucleic acid scavenging capacity and *in vivo* functionality of PAMAM G3 while avoiding the cellular and most aspects of the *in vivo* toxicity associated with the administration of the fully cationic PAMAMs.

While the generational increase in cationic PAMAM toxicity is well recognized,[14,15,20,21] the toxicity of PAMAM generations smaller than four has been less explored. *In vivo* toxicity data for unmodified, low-generation PAMAM dendrimers are even more limited, particularly when the compounds are administered as free molecules not complex with nucleic acids before injection. Unlike the initial *in vivo* studies of PAMAM, which suggested that low-generation cationic PAMAMs have limited toxicity,[14] our group and others have shown that cationic PAMAM G3 has significant *in vivo* toxicity, including embryonic toxicity, weight loss, and skin necrosis.[12,17,22] In fact, to evaluate the effects of PAMAM G3 in mice, we first established the LD50 to be 100-200 mg/kg and utilized the compound at a 5- to 10-fold reduced concentration below this level for efficacy studies.[8] This study recapitulates these findings by demonstrating generation- and dose-dependent *in vitro* cytotoxicity and *in vivo* toxicity in the form of weight loss and abnormalities in liver and kidney function tests at the 20-40 mg/kg dose. Furthermore, our histopathologic findings of substantial intraperitoneal surface inflammation following the IP injection of PAMAM G3 suggest that one

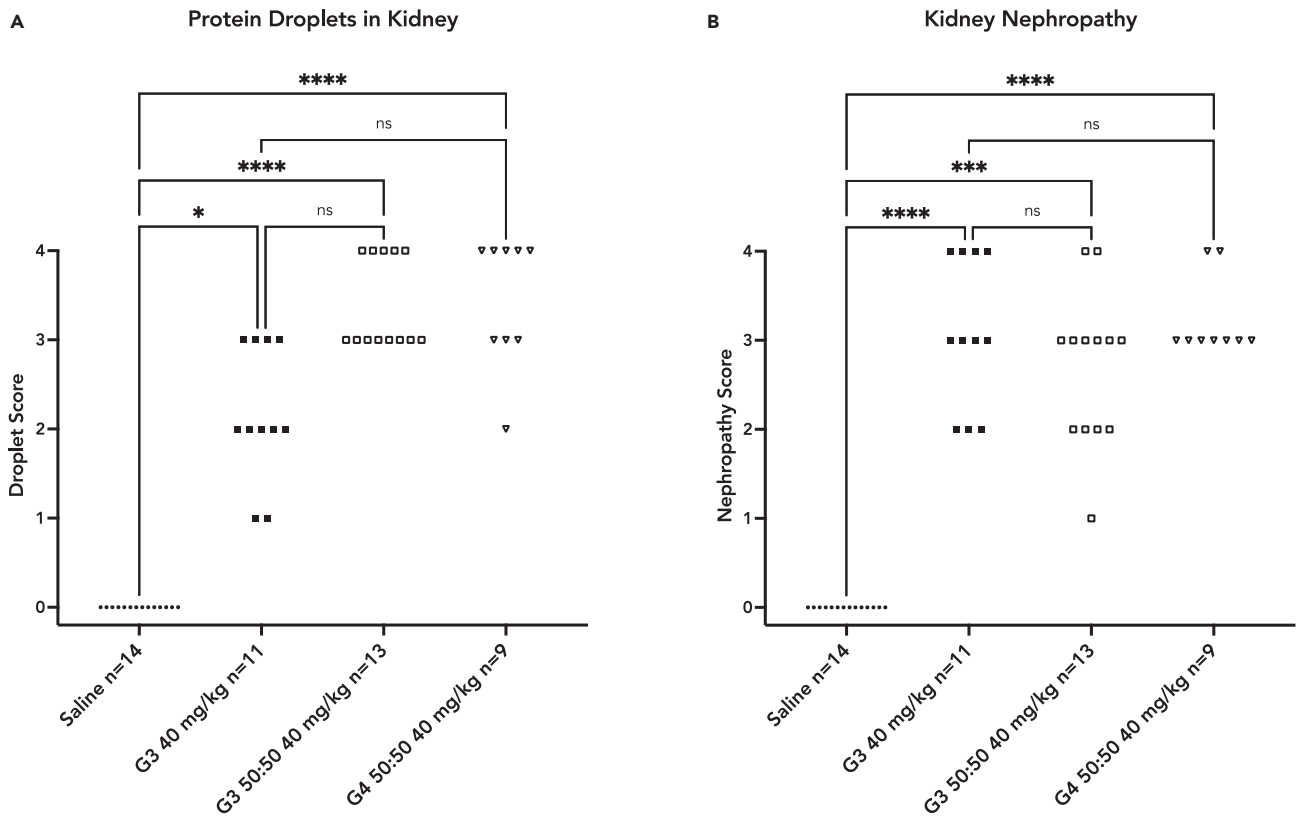

Figure 11. Protein droplets and nephropathic changes are evident in the kidneys of mice treated short term at 40 mg/kg with cationic and with mixed surface PAMAM scavengers

(A) Protein droplet scores across treatment groups.

(B) Nephropathy scores across treatment groups.

Treatments were compared using the Kruskal-Wallis test followed by post hoc analysis via Dunn's multiple comparisons test. Significance: * represents $p = 0.0277$, *** represents $p = 0.00030$, and **** represents $p \leq 0.0001$. See also Figures S5 and S6.

mechanism of PAMAM's *in vivo* toxicity is a direct, contact-induced damage to cellular membranes, which worsens with the increasing density of each generation's cationic surface charge. These findings also contextualize the contrasting reports of lethal thrombotic events following intravenous injection of cationic PAMAM G4 in healthy mice but the anticoagulant effect of G3 in vascular injury models.[23,24] Following injury, the large circulating number of procoagulant DAMPs released from the vascular endothelium, activated platelets or neutrophils are bound and sequestered by the positive surface charges of the scavenger. In the uninjured mouse, those unshielded charges can cause direct toxicity to the vascular endothelium, exposing the procoagulant DAMPs and subendothelium. In this regard, we have observed that diseased animals often tolerate DAMP/PAMP scavenger treatment better than healthy normal control animals just as the treatment of cells in culture with cationic polymers bound to DNA or RNA often shows less toxicity than when cells are treated with cationic polymers alone.

This study also provides important biodistribution and excretion data for low-generation PAMAMs. While studies of radiolabeled PAMAM have suggested kidney filtration and urinary excretion of smaller generation PAMAM and liver metabolism and distributed visceral organ distribution of generations 4 and larger,[25,26] we have not found any other study that examined kidney histology in detail following treatment with low-generation PAMAM. We report that treatment with PAMAM G3, or either of the mixed surface dendrimers, G3 50:50 and G4 50:50, results in the deposition of protein droplets and nephropathic changes in the renal tubules in normal healthy mice. Interestingly, these changes do not correlate with serum kidney function tests in animals treated with the mixed PAMAM variants even though they do for the fully cationic PAMAMs. The tubular epithelial changes are reminiscent of hydrocarbon nephropathy in rodents where the compound binds to proteins in proximal tubules and results in lysosomal overload, cell death, and resultant cell proliferation.

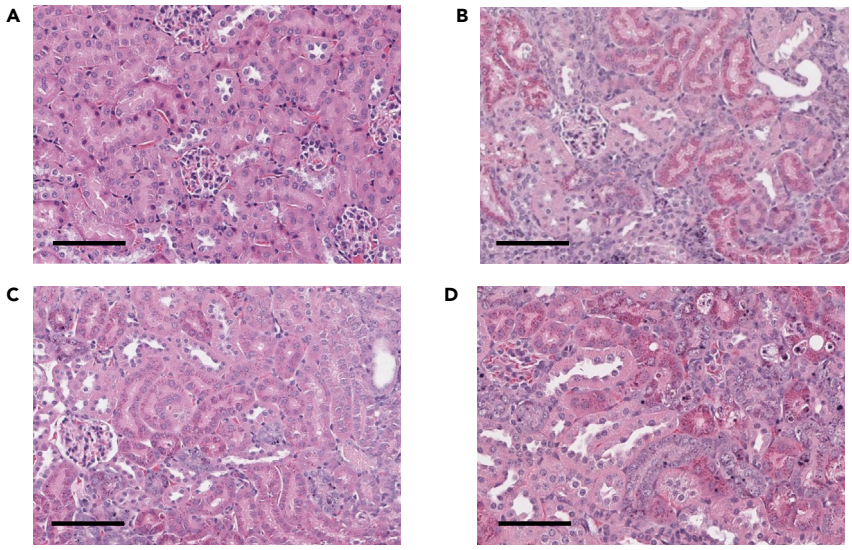

Figure 12. Photomicrographs of eosinophilic protein droplets and tubular nephropathic changes in the renal cortices of mice treated short term at 40 mg/kg with cationic and with mixed surface PAMAM scavengers

(A) Normal renal proximal tubules in saline-treated mouse.
(B) Kidney of G3-treated mouse.
(C) Kidney of G3 50:50-treated mouse.
(D) Kidney of G4 50:50-treated mouse.
Bar indicates 100 μM.

Although no mechanism can be inferred from the renal lesions in the current study, it would be of interest to examine protein-compound interactions and to see what tubular epithelial organelles are affected. Moreover, it will be important to determine if such protein droplets are less likely to form if high levels of nucleic acid-containing DAMPs are present and block such protein interactions with the free polymers.

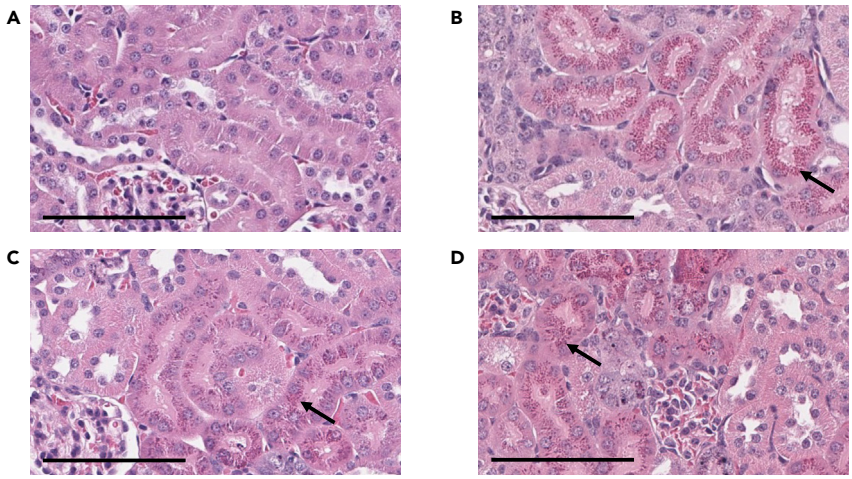

Figure 13. High magnification photomicrographs of eosinophilic protein droplets and tubular nephropathic changes in the renal cortices of mice treated short term at 40 mg/kg with cationic and with mixed surface PAMAM scavengers

(A) High magnification image of normal renal proximal tubules in saline-treated mouse.
(B) High magnification image of kidney of G3-treated mouse.
(C) High magnification image of kidney of G3 50:50-treated mouse.
(D) High magnification image of kidney of G4 50:50-treated mouse.
Arrows identify eosinophilic protein droplets. Bar indicates 100 μM.

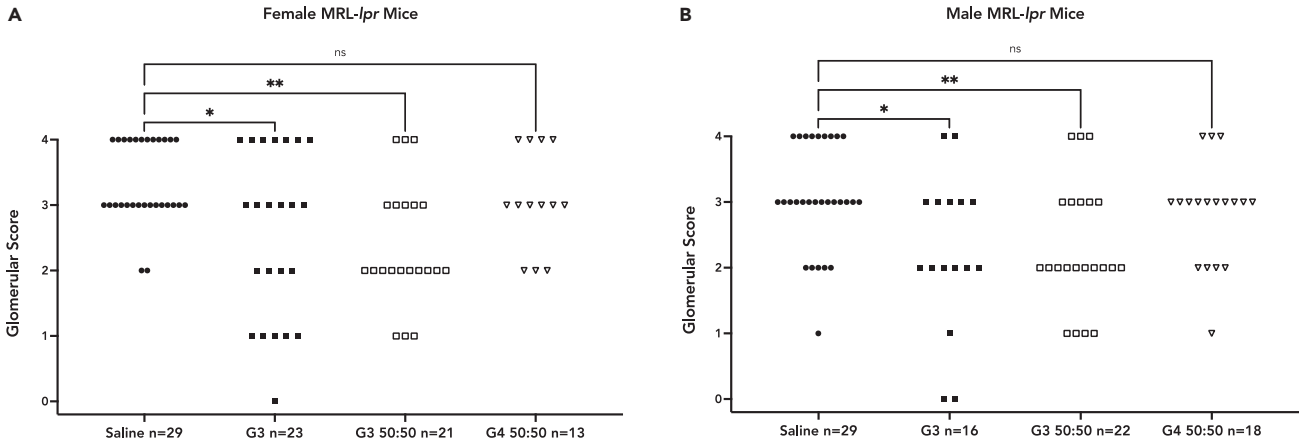

Figure 14. Treatment with G3 and the mixed surface scavenger G3 50:50 reduce glomerular nephritis in lupus-prone MRL-*lpr* mice compared to saline or G4 50:50 treatments

(A) Female mice.

(B) Male mice.

For each sex, the Kruskal-Wallis nonparametric test was applied followed by post hoc evaluation via Dunn's multiple comparisons test with each polymer treatment compared to the saline control. Significance: for female mice * represents p = 0.0441, ** represents p = 0.0014; for male mice * represents p = 0.0376 and ** represents p = 0.0100.

While the mechanism by which PAMAM G3 50:50 slows the progression of glomerulonephritis in murine lupus is not completely defined, previous work has shown that PAMAM G3 can prevent complex formation by sequestering DNA and other negatively charged nuclear antigens, blocking their interactions with autoantibodies *in vitro*[13]; our studies herein reveal that PAMAM G3 50:50 can also capture DNA and compete with anti-DNA antibody binding albeit less efficiently than the fully modified variant. Since lupus nephritis is driven in part by a TLR-mediated glomerular and tubulointerstitial inflammatory response to renally deposited immune complexes,[27] nucleic acid-DAMP scavengers may also modulate complex-driven inflammation in the kidney itself. In this study, we found that the mixed surface PAMAM G3 50:50 scavenges nucleic acid-based TLR agonists comparably to fully modified PAMAM variants (Figure 1) and significantly reduces glomerulonephritis (Figures 14 and 15).

In summary, we report that mixed-surface PAMAM variants are able to bind and neutralize pro-inflammatory nucleic acid-DAMPs in TLR activation assays equivalently to purely cationic polymers with the same number of positive charges with markedly reduced cellular toxicity. *In vivo*, these mixed-surface polymer

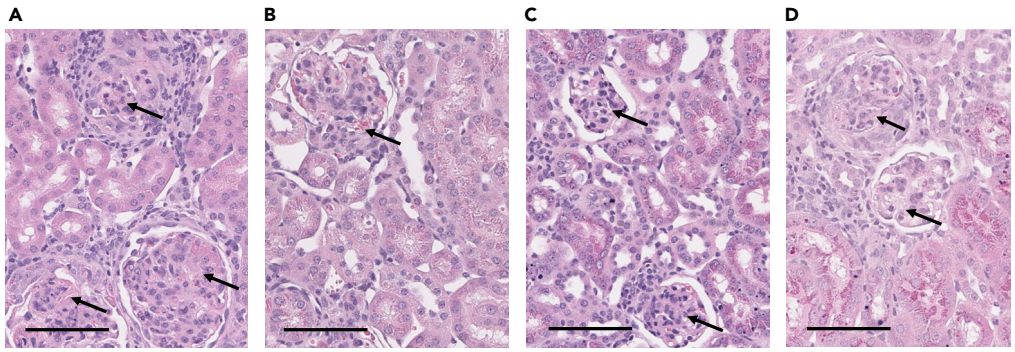

Figure 15. Photomicrographs showing the reduction of glomerulonephritis in lupus prone MRL-*lpr* mice after treatment with G3 and G3 50:50

(A) Kidney of female saline-treated mouse.

(B) Kidney of female G3-treated mouse.

(C) Kidney of female G3 50:50-treated mouse.

(D) Kidney of female G4 50:50-treated mouse. Arrows denote glomeruli. Bar indicates 100 μM.

variants induce less weight loss and resolve the serosal inflammatory organ injury seen with the use of purely cationic PAMAM G3. In addition, the mixed surface polymer G3 50:50 relieves glomerulonephritis in lupus-prone MRL-*lpr* mice as well or better than fully cationic G3. This study also presents important *in vivo* toxicology data for the low-generation cationic PAMAMs, which are broadly considered to be non-toxic and biocompatible even when administered alone and not as a complex with nucleic acid. Collectively, these data reveal that mixed-surface PAMAMs represent a new class of nucleic acid scavengers with inhibitory activity and improved biocompatibility. Thus, the translational development of anti-inflammatory dendrimers is increasingly feasible for lupus and other indications where nucleic acid-DAMP scavenging has shown benefits including autoimmune diseases such as psoriasis,[28,29] rheumatoid arthritis,[30,31] and inflammatory bowel disease,[32] as well as infectious diseases, such as influenza, sepsis[33,34] and COVID-19,[35] and cancer.[9–11]

Limitations of study

Potential limitations include the artificial nature of the prototypic TLR agonists used and relying on a single animal model of lupus. Moreover, the treatment strategy utilized starts therapy at a relatively young age. Thus, the approach evaluates the use of nucleic acid scavengers to limit the development of lupus nephritis and not whether advanced lupus disease when already present can be effectively treated. In addition, the inbred nature of the animal model used in the study represents only certain pathways for autoimmunity and will not fully recapitulate the diverse set of disease determinants that will be encountered in the human lupus patient population. Finally, the toxicity studies reported only evaluated a treatment regimen of 4 doses delivered every three days in young healthy mice. Other dosing regimens over longer or shorter time periods in aged or diseased animals may result in different levels of toxicity.

STAR★METHODS

Detailed methods are provided in the online version of this paper and include the following:

- KEY RESOURCES TABLE
- RESOURCE AVAILABILITY
  - Lead contact
  - Materials availability
  - Data and code availability
- EXPERIMENTAL MODEL AND SUBJECT DETAILS
  - Animal studies
  - Cell lines
- METHOD DETAILS
  - Polymer design, production, and preparation
  - TLR activation assays
  - Isothermal titration calorimetry (ITC)
  - Enzyme-linked immunosorbent assays (ELISAs)
  - Polymer capture ELISAs
  - Polymer blocking, competition and displacement ELISAs
  - Cell toxicity assays
  - General notes on the studies in mice
  - Short term toxicity studies in mice
  - Analysis of inflammatory cytokines using LEGENDplex
  - Recovery Study in mice
  - SLE long term treatment
- QUANTIFICATION AND STATISTICAL ANALYSIS

SUPPLEMENTAL INFORMATION

Supplemental information can be found online at https://doi.org/10.1016/j.isci.2022.105542.

ACKNOWLEDGMENTS

This work was supported by the National Institutes of Health grant RO1AR073935 (to B.A.S. and D.S.P.) and by the Medical Research Service, Veterans Administration (to D.S.P). We thank Emery Scheibert and Mark Kaiser of Dendritech, Inc. for helpful discussions on the possibilities for altering dendrimer characteristics

and arranging for the synthesis of the mixed surface PAMAM variants. We also thank Linsley Kelly for extensive discussions about the therapeutic window for nucleic acid scavengers and George Pitoc for assistance with mouse protocols. The graphical abstract was created with BioRender.com.

AUTHOR CONTRIBUTIONS

Conceptualization, L.B.O., J.I.E., and B.A.S.; formal analysis, L.B.O., R.E.R., H.Y., C.Z.S. and S.A.E.; investigation, L.B.O., N.I.H., R.E.R., W.S.G, and J.I.E.; resources, A.K.V., D.M.S., A.C., B.A.S.; writing – original draft, L.B.O., R.E.R., H.Y., J.I.E.; writing – review and editing, L.B.O., N.I.H, R.E.R., H.Y., J.I.E., and B.A.S.; visualization, L.B.O., N.I.H., R.E.R., H.Y., J.I.E.; supervision, A.C., D.S.P., and B.A.S.; funding acquisition, B.A.S. and D.S.P.

DECLARATION OF INTERESTS

Duke University has applied for patents on the strategy to reduce inflammation via nucleic acid scavengers. Lyra Olson, Nicole Hunter, Rachel Rempel, and Bruce Sullenger are listed as inventors on such patents.

Received: April 8, 2022
Revised: June 2, 2022
Accepted: November 7, 2022
Published: December 22, 2022

REFERENCES

1. Anders, H.-J., and Schaefer, L. (2014). Beyond tissue injury-damage-associated molecular patterns, toll-like receptors, and inflammasomes also drive regeneration and fibrosis. J. Am. Soc. Nephrol. *25*, 1387–1400. https://doi.org/10.1681/ASN.2014010117.

2. Wu, Y.-w., Tang, W., and Zuo, J.-p. (2015). Toll-like receptors: potential targets for lupus treatment. Acta Pharmacol. Sin. *36*, 1395–1407. https://doi.org/10.1038/aps.2015.91.

3. Gao, W., Xiong, Y., Li, Q., and Yang, H. (2017). Inhibition of toll-like receptor signaling as a promising therapy for inflammatory diseases: a journey from molecular to Nano therapeutics. Front. Physiol. *8*, 508. https://doi.org/10.3389/fphys.2017.00508.

4. Tomalia, D.A., Baker, H., Dewald, J., Hall, M., Kallos, G., Martin, S., Roeck, J., Ryder, J., and Smith, P. (1985). A new class of polymers: starburst-dendritic macromolecules. Polym. J. *17*, 117–132. https://doi.org/10.1295/polymj.17.117.

5. Lee, J., Sohn, J.W., Zhang, Y., Leong, K.W., Pisetsky, D., and Sullenger, B.A. (2011). Nucleic acid-binding polymers as anti-inflammatory agents. Proc. Natl. Acad. Sci. USA *108*, 14055–14060. https://doi.org/10.1073/pnas.1105777108.

6. Anwar, M.A., Shah, M., Kim, J., and Choi, S. (2019). Recent clinical trends in Toll-like receptor targeting therapeutics. Med. Res. Rev. *39*, 1053–1090. https://doi.org/10.1002/med.21553.

7. Holl, E.K., Bond, J.E., Selim, M.A., Ehanire, T., Sullenger, B., and Levinson, H. (2014). The nucleic acid scavenger polyamidoamine third-generation dendrimer inhibits fibroblast activation and granulation tissue contraction. Plast. Reconstr. Surg. *134*, 420e–433e. https://doi.org/10.1097/PRS.0000000000000471.

8. Holl, E.K., Shumansky, K.L., Borst, L.B., Burnette, A.D., Sample, C.J., Ramsburg, E.A., and Sullenger, B.A. (2016). Scavenging nucleic acid debris to combat autoimmunity and infectious disease. Proc. Natl. Acad. Sci. USA *113*, 9728–9733. https://doi.org/10.1073/pnas.1607011113.

9. Naqvi, I., Gunaratne, R., McDade, J.E., Moreno, A., Rempel, R.E., Rouse, D.C., Herrera, S.G., Pisetsky, D.S., Lee, J., White, R.R., and Sullenger, B.A. (2018). Polymer-mediated inhibition of pro-invasive nucleic acid DAMPs and microvesicles limits pancreatic cancer metastasis. Mol. Ther. *26*, 1020–1031. https://doi.org/10.1016/j.ymthe.2018.02.018.

10. Eteshola, E.O.U., Landa, K., Rempel, R.E., Naqvi, I.A., Hwang, E.S., Nair, S.K., and Sullenger, B.A. (2021). Breast cancer-derived DAMPs enhance cell invasion and metastasis, while nucleic acid scavengers mitigate these effects. Mol. Ther. Nucleic Acids *26*, 1–10. https://doi.org/10.1016/j.omtn.2021.06.016.

11. Holl, E.K., Frazier, V., Landa, K., Boczkowski, D., Sullenger, B., and Nair, S.K. (2021). Controlling cancer-induced inflammation with a nucleic acid scavenger prevents lung metastasis in murine models of breast cancer. Mol. Ther. *29*, 1772–1781. https://doi.org/10.1016/j.ymthe.2020.12.026.

12. Kelly, L., Olson, L.B., Rempel, R.E., Everitt, J.I., Levine, D., Nair, S.K., Davis, M.E., and Sullenger, B.A. (2022). beta-Cyclodextrin-containing polymer treatment of cutaneous lupus and influenza improves outcomes. Mol. Ther. *30*, 845–854. https://doi.org/10.1016/j.ymthe.2021.10.003.

13. Stearns, N.A., Lee, J., Leong, K.W., Sullenger, B.A., and Pisetsky, D.S. (2012). The inhibition of anti-DNA binding to DNA by nucleic acid binding polymers. PLoS One *7*, e40862. https://doi.org/10.1371/journal.pone.0040862.

14. Roberts, J.C., Bhalgat, M.K., and Zera, R.T. (1996). Preliminary biological evaluation of polyamidoamine (PAMAM) StarburstTM dendrimers. J. Biomed. Mater. Res. *30*, 53–65. https://doi.org/10.1002/(SICI)1097-4636(199601)30:1<53::AID-JBM8>3.0.CO;2-Q.

15. Malik, N., Wiwattanapatapee, R., Klopsch, R., Lorenz, K., Frey, H., Weener, J.W., Meijer, E.W., Paulus, W., and Duncan, R. (2000). Dendrimers:: relationship between structure and biocompatibility in vitro, and preliminary studies on the biodistribution of 125I-labelled polyamidoamine dendrimers in vivo. J. Contr. Release *65*, 133–148. https://doi.org/10.1016/S0168-3659(99)00246-1.

16. Chauhan, A.S., Diwan, P.V., Jain, N.K., and Tomalia, D.A. (2009). Unexpected in vivo anti-inflammatory activity observed for simple, surface functionalized poly (amidoamine) dendrimers. Biomacromolecules *10*, 1195–1202. https://doi.org/10.1021/bm9000298.

17. Heiden, T.C.K., Dengler, E., Kao, W.J., Heideman, W., and Peterson, R.E. (2007). Developmental toxicity of low generation PAMAM dendrimers in zebrafish. Toxicol. Appl. Pharmacol. *225*, 70–79. https://doi.org/10.1016/j.taap.2007.07.009.

18. Tang, Y., Han, Y., Liu, L., Shen, W., Zhang, H., Wang, Y., Cui, X., Wang, Y., Liu, G., and Qi, R. (2015). Protective effects and mechanisms of G5 PAMAM dendrimers against acute pancreatitis induced by caerulein in mice. Biomacromolecules *16*, 174–182. https://doi.org/10.1021/bm501390d.

19. Dufour, J.H., Dziejman, M., Liu, M.T., Leung, J.H., Lane, T.E., and Luster, A.D. (2002). IFN-gamma-inducible protein 10 (IP-10; CXCL10)-deficient mice reveal a role for IP-10 in

effector T cell generation and trafficking. J. Immunol. *168*, 3195–3204. https://doi.org/10.4049/jimmunol.168.7.3195.

20. Jain, K., Kesharwani, P., Gupta, U., and Jain, N.K. (2010). Dendrimer toxicity: let's meet the challenge. Int. J. Pharm. *394*, 122–142. https://doi.org/10.1016/j.ijpharm.2010.04.027.

21. Fox, L.J., Richardson, R.M., and Briscoe, W.H. (2018). PAMAM dendrimer - cell membrane interactions. Adv. Colloid Interface Sci. *257*, 1–18. https://doi.org/10.1016/j.cis.2018.06.005.

22. Pryor, J.B., Harper, B.J., and Harper, S.L. (2014). Comparative toxicological assessment of PAMAM and thiophosphoryl dendrimers using embryonic zebrafish. Int. J. Nanomed. *9*, 1947–1956. https://doi.org/10.2147/IJN.S60220.

23. Jain, S., Pitoc, G.A., Holl, E.K., Zhang, Y., Borst, L., Leong, K.W., Lee, J., and Sullenger, B.A. (2012). Nucleic acid scavengers inhibit thrombosis without increasing bleeding. Proc. Natl. Acad. Sci. USA *109*, 12938–12943. https://doi.org/10.1073/pnas.1204928109.

24. Greish, K., Thiagarajan, G., Herd, H., Price, R., Bauer, H., Hubbard, D., Burckle, A., Sadekar, S., Yu, T., Anwar, A., et al. (2012). Size and surface charge significantly influence the toxicity of silica and dendritic nanoparticles. Nanotoxicology *6*, 713–723. https://doi.org/10.3109/17435390.2011.604442.

25. Lesniak, W.G., Mishra, M.K., Jyoti, A., Balakrishnan, B., Zhang, F., Nance, E., Romero, R., Kannan, S., and Kannan, R.M. (2013). Biodistribution of fluorescently labeled PAMAM dendrimers in neonatal rabbits: effect of neuroinflammation. Mol. Pharm. *10*, 4560–4571. https://doi.org/10.1021/mp400371r.

26. Labieniec-Watala, M., and Watala, C. (2015). PAMAM dendrimers: destined for success or doomed to fail? Plain and modified PAMAM dendrimers in the context of biomedical applications. J. Pharmacol. Sci. *104*, 2–14. https://doi.org/10.1002/jps.24222.

27. Davidson, A., Berthier, C., and Kretzler, M. (2013). Chapter 18 - pathogenetic mechanisms in lupus nephritis. In Dubois' Lupus Erythematosus and Related Syndromes (Eighth Edition), D.J. Wallace and B.H. Hahn, eds. (W.B. Saunders), pp. 237–255. https://doi.org/10.1016/B978-1-4377-1893-5.00018-2.

28. Liang, H., Yan, Y., Wu, J., Ge, X., Wei, L., Liu, L., and Chen, Y. (2020). Topical nanoparticles interfering with the DNA-LL37 complex to alleviate psoriatic inflammation in mice and monkeys. Sci. Adv. *6*, eabb5274. https://doi.org/10.1126/sciadv.abb5274.

29. Yan, Y., Liang, H., Liu, X., Liu, L., and Chen, Y. (2021). Topical cationic hairy particles targeting cell free DNA in dermis enhance treatment of psoriasis. Biomaterials *276*, 121027. https://doi.org/10.1016/j.biomaterials.2021.121027.

30. Peng, B., Liang, H., Li, Y., Dong, C., Shen, J., Mao, H.Q., Leong, K.W., Chen, Y., and Liu, L. (2019). Tuned cationic dendronized polymer: molecular scavenger for rheumatoid arthritis treatment. Angew Chem. Int. Ed. Engl. *58*, 4254–4258. https://doi.org/10.1002/anie.201813362.

31. Liang, H., Peng, B., Dong, C., Liu, L., Mao, J., Wei, S., Wang, X., Xu, H., Shen, J., Mao, H.Q., et al. (2018). Cationic nanoparticle as an inhibitor of cell-free DNA-induced inflammation. Nat. Commun. *9*, 4291. https://doi.org/10.1038/s41467-018-06603-5.

32. Shi, C., Dawulieti, J., Shi, F., Yang, C., Qin, Q., Shi, T., Wang, L., Hu, H., Sun, M., Ren, L., et al. (2022). A nanoparticulate dual scavenger for targeted therapy of inflammatory bowel disease. Sci. Adv. *8*, eabj2372. https://doi.org/10.1126/sciadv.abj2372.

33. Dawulieti, J., Sun, M., Zhao, Y., Shao, D., Yan, H., Lao, Y.H., Hu, H., Cui, L., Lv, X., Liu, F., et al. (2020). Treatment of severe sepsis with nanoparticulate cell-free DNA scavengers. Sci. Adv. *6*, eaay7148. https://doi.org/10.1126/sciadv.aay7148.

34. Liu, F., Sheng, S., Shao, D., Xiao, Y., Zhong, Y., Zhou, J., Quek, C.H., Wang, Y., Hu, Z., Liu, H., et al. (2021). A cationic metal-organic framework to scavenge cell-free DNA for severe sepsis management. Nano Lett. *21*, 2461–2469. https://doi.org/10.1021/acs.nanolett.0c04759.

35. Naqvi, I., Giroux, N., Olson, L., Morrison, S.A., Llanga, T., Akinade, T.O., Zhu, Y., Zhong, Y., Bose, S., Arvai, S., et al. (2022). DAMPs/PAMPs induce monocytic TLR activation and tolerance in COVID-19 patients; nucleic acid binding scavengers can counteract such TLR agonists. Biomaterials *283*, 121393. https://doi.org/10.1016/j.biomaterials.2022.121393.

36. Meyerholz, D.K., Tintle, N.L., and Beck, A.P. (2019). Common pitfalls in analysis of tissue scores. Vet. Pathol. *56*, 39–42. https://doi.org/10.1177/0300985818794250.

STAR★METHODS

KEY RESOURCES TABLE

REAGENT or RESOURCE	SOURCE	IDENTIFIER
Antibodies		
Val-1205	Valerion Therapeutics	Stock #: VALE-915
Anti-Human Ig-G (γ-chain specific) – peroxidase antibody produced in goat	Millipore Sigma	Cat#: A6029; RRID: AB_258272; Lot#: SLCG4694
Biological samples		
Calf thymus DNA	Worthington Biochemical Corporation	Cat#: LS002105
Chemicals, peptides, and recombinant proteins		
PAMAM G2	Dendritech, Inc.	Lot#: 0618-17-E2.0-LD-W; http://www.dendritech.com/pricing.html
PAMAM G3 50:50	Dendritech, Inc.	Lot#: 0820-04-E3.0-LD(50% OH); http://www.dendritech.com/pricing.html
PAMAM G3	Dendritech, Inc.	Lot#: 1020-02-E3.0-LD; http://www.dendritech.com/pricing.html
PAMAM G4 50:50	Dendritech, Inc.	Lot#: 1019-11-E4.0-LD(50% OH); http://www.dendritech.com/pricing.html
PAMAM G4	Dendritech, Inc.	Lot#: 1019-20-E4.0-LD; http://www.dendritech.com/pricing.html
Lipopolysaccharide	InvivoGen	Cat#: tlrl-b5lps
Critical commercial assays		
CellTiter-Glo® luminescent cell viability assay	Promega	Cat#: G7570
QUANTI-blue	InvivoGen	Cat#: rep-qbs
LEGENDplex™ Multi-Analyte Flow Assay Kit, Mouse Anti-Virus Response Panel (13-plex) with V-Bottom Plate	BioLegend	Cat#: 740622
Deposited data		
Raw and analyzed data	This paper	Available from Corresponding author - Sullenger
Experimental models: Cell lines		
HEK-Blue hTLR 3	InvivoGen	Cat#: hkb-htlr3; RRID: CVCL_IM81
HEK-Blue hTLR 4	InvivoGen	Cat#: hkb-htlr4; RRID: CVCL_IM82
HEK-Blue hTLR 7	InvivoGen	Cat#:hkb-htlr7; RRID: CVCL_IM84
HEK-Blue hTLR 9	InvivoGen	Cat#: hkb-htlr9; RRID: CVCL_IM86
RAW 264.7	American Type Culture Collection	Cat#: TIB-71; RRID: CVCL_0493
Experimental models: Organisms/strains		
Mouse: C57BL/6J	The Jackson Laboratory	Cat#: 000664; RRID: IMSR_JAX:000664
Mouse: MRL-*lpr*: MRL/MpJ-*Fas*^{lpr}/J	The Jackson Laboratory	Cat#: 000485; RRID: IMSR_JAX:000485
Oligonucleotides		
CpG 1668 5′-TCCATGACGTTCCTGATGCT-3′	InvivoGen	Cat#: tlrl-1668
High Molecular Weight Poly (I:C)	InvivoGen	Cat#: tlrl-pic

(*Continued on next page*)

Continued

REAGENT or RESOURCE	SOURCE	IDENTIFIER
Software and algorithms		
ITCRun	TA Instruments	https://www.tainstruments.com/itcrun-dscrun-nanoanalyze-software/
NanoAnalyze	TA Instruments	https://www.tainstruments.com/itcrun-dscrun-nanoanalyze-software/
GraphPad Prism v9.4.1	GraphPad	https://www.graphpad.com/scientific-software/prism/
LEGENDplex™ v8 Data Analysis Software	BioLegend	https://www.biolegend.com/en-us/legendplex

RESOURCE AVAILABILITY

Lead contact

Further information and requests for resources and reagents should be directed to and will be fulfilled by the lead contact, Bruce Sullenger (bruce.sullenger@duke.edu).

Materials availability

Two mixed surface PAMAM variants were synthesized as a custom order for us by Dendritech, Inc.: G3 50:50 (16 terminal amines, 16 terminal hydroxyls, ~6.9 kD), and G4 50:50 (32 terminal amines, 32 terminal hydroxyls, ~14.2 kD).

Data and code availability

- All data reported in this paper will be shared by the lead contact upon request.
- This paper does not report original code.
- Any additional information required to reanalyze the data reported in this paper is available from the lead contact upon request.

EXPERIMENTAL MODEL AND SUBJECT DETAILS

Animal studies

Short term and recovery toxicity studies

Female C57BL/6J mice (RRID: IMSR_JAX:000664) were obtained from The Jackson Laboratory. Mice were purchased at eight weeks of age and allocated to cages at a density of four to five mice per cage. At ten weeks of age mice were ear punched for identification, weighed, and treatment regimens initiated. At all times, mice received food and water *ad libitum*. Studies were conducted in accordance with the Guide for the Care and Use of Laboratory Animals (National Research Council, 2011) and approved by the Duke University Institutional Animal Care and Use Committee (Protocols A201-18-08 and A156-21-07).

SLE long term treatment study

Male and female MRL-*lpr* mice (RRID: IMSR_JAX:000485) were obtained from The Jackson Laboratory to establish a breeding colony. Mice of this strain are homozygous for the lymphoproliferation spontaneous mutation *Fas*^{lpr}. Purchased female breeder mice produced up to two litters before debilitation from lupus, upon which they were euthanized. Purchased male breeders had had somewhat later onset of lupus, and were euthanized upon debilitation. The MRL-*lpr* progeny were weaned at three weeks, males and females separated, housed at a density of four mice per cage with random assignment of littermates, and aged. Upon reaching the age of nine weeks for females and ten weeks for males, the mice were ear punched for identification, weighed, and treatment regimens initiated. Approximately every four weeks, due to enhanced healing that fills in the ear punch, mice were ear punched again to maintain their identification marking. At all times, mice received food and water *ad libitum*. The study was conducted in accordance with the Guide for the Care and Use of Laboratory Animals (National Research Council, 2011) and approved by the Duke University Institutional Animal Care and Use Committee (Protocols A201-18-08 and A156-21-07).

Cell lines

TLR activation assays and cell toxicity assays

HEK-Blue hTLR 3, 4, 7, and 9 cells (RRID: CVCL_IM81, CVCL_IM82, CVCL_IM84, CVCL_IM86) derived from the human female HEK293 line were purchased from InvivoGen and maintained in culture according to manufacturer's instructions using a growth media of DMEM, 4.5 g/L glucose, 2 mM L-glutamine, 10% (v/v) fetal bovine serum, 100 U/mL penicillin, 100 μg/mL streptomycin, 100 μg/mL Normocin™. The RAW 264.7 macrophage cell line (RRID: CVCL_0493), derived from ascites induced by infection with the Abelson murine leukemia virus of a male BALB/c mouse, was purchased from the American Type Culture Collection through the Duke CCF Cell Lines Core. RAW 264.7 cells were maintained in culture according to collection's instructions using a growth media of DMEM with 4.5 g/L glucose, 2 mM L-glutamine, sodium pyruvate, and sodium bicarbonate (Sigma D6429-500 mL) supplemented with 10% FBS (not heat inactivated). All cells were grown at 37°C in 5% CO2 at 95% relative humidity.

METHOD DETAILS

Polymer design, production, and preparation

Three whole generation cationic polyamidoamine polymers, abbreviated as PAMAMs, were acquired from Dendritech, a commercial manufacturer and supplier of this dendrimer family: G2 (16 terminal amines, ~3.3 kD), G3 (32 terminal amines, ~6.9 kD, and G4 (64 terminal amines, ~14.2 kD). These dendrimers are made by repetitive reactions of ethylenediamine and methyl acrylate to build an organized, highly uniform polymer with low polydispersity and a large number of terminal groups on the dendrimer surface. Two mixed surface PAMAM variants were synthesized as a custom order for us by Dendritech, Inc.: G3 50:50 (16 terminal amines, 16 terminal hydroxyls, ~6.9 kD), and G4 50:50 (32 terminal hydroxyls, ~14.2 kD) (Figure S1). In contrast to the usual terminal primary amine surfaces, mixed surfaces can be made that incorporate monoethanolamine in the process, resulting in both primary amidoamine (-NH2) and amidoalcohol (-OH) surface groups. These mixed surfaces can be produced in any desired ratio to tailor the performance properties of the dendrimers for a particular application. The functional groups are statistically distributed across the dendrimer surface, hence the descriptor "mixed" surfaces. Polymers were characterized by ^{13}C NMR to confirm average distribution value.

Polymers were kept lyophilized at −80°C for long term storage. In preparation for use they were resuspended to 100 mg/mL in sterile dH_2O and stored at 4° protected from light. On each day of mouse treatment, polymers were dispersed into 3 mg/mL or 6 mg/mL working solutions with sterile physiological saline and filtered through a 0.2 micron RC membrane filter (VWR Avantor cat#: 28200-024).

TLR activation assays

HEK-Blue hTLR 3, 4, and 9 cells were plated for activation assays in 96-well plates at 40,000 cells per well and allowed to settle overnight. Canonic agonists, high molecular weight Poly(I:C) (1 μg/mL), CpG 1668 oligonucleotide (1 μM), and lipopolysaccharide (LPS-B5, 1 ng/mL) for hTLR 3, 9 and 4 respectively, were purchased from InvivoGen and resuspended according to manufacturer's instructions. Media were then removed and fresh media including control agonists and varying concentrations of polymer in 100 μL total volume were added and allowed to incubate for 24 h. With no polymer addition the pH of the DMEM medium was pH 7.3. As concentrations of G3, G3 50:50 and G4 50:50 rose, the associated pHs rose as well, but essentially in parallel. For instance, at the 16 μM concentrations the associated pHs were close to 7.6 and at the 32 μM concentrations the associated pHs remained similar to each other at around pH 7.7. After incubation, 40 μL of supernatant was removed from each well to a fresh 96 well plate. Quantiblue (InvivoGen) was resuspended according to manufacturer's instructions, 160 μL was added to wells and incubated for 3 h at 37°C. The absorbance of the wells was read at 655 nM on a Spectramax i3 (Molecular Devices) plate reader and data presented as percent of maximum activation with canonic agonist alone with each data point the mean of three technical replicates.

Isothermal titration calorimetry (ITC)

Isothermal titration calorimetry for assessing polymer and DNA interactions was conducted using the Nano ITC calorimeter and associated program ITCRun from TA Instruments. Reagents were prepared in PBS without calcium chloride and magnesium chloride (Sigma cat#: D8537). The reference cell was filled with 1 mL PBS. The nucleic acid was the CpG ODN 1668 (InvivoGen cat#: tlrl-1668) and, as outlined above, the polymers were sourced from Dendritech. One milliliter of nucleic acid in PBS (solution pH 7.2)

was loaded into the sample cell and polymer in PBS (solution pH 7.3) was titrated into the cell at 10 μL per injection at a stirring rate of 350 rpm for a total of 25 injections at room temperature (25°C). Spacing between injections was set to 240 s for the solution to reach equilibrium. Titrations of each polymer into the sample cell filled with plain PBS were performed to determine the background heat of dilution for the polymers. For the assessment of PAMAM G3 binding to DNA, the polymer was at 37.5 μM in the injection syringe and the oligo was at 13.158 μM in the sample cell. For the assessment of PAMAM G3 50:50 binding to DNA, the polymer was at 62.5 μM in the injection syringe and the oligo was at 13.158 μM in the sample cell. For the assessment of PAMAM G4 50:50 binding to DNA, the polymer was at 37.5 μM in the injection syringe and the oligo was at 10.526 μM in the sample cell. Calorimetry results were fitted using the TA Instruments provided program NanoAnalyze. For each analysis, the first injection value was omitted and background was removed by applying a linear model generated by the titration of each polymer to the PBS buffer. The thermograms were then fitted using a multiple site binding model constrained to two-sites.

Enzyme-linked immunosorbent assays (ELISAs)

All ELISA experiments used Immulon 2HB (high binding) flat-bottom, 96 well microtiter plates (Thermofisher 3455, VWR cat# 62402-972). Typically, samples had a final volume of 100 μL/well with incubations at room temperature for 1 h. Washes used phosphate buffered saline (PBS) free of cations at room temperature. Blocking used 200 μL/well of 2% bovine serum albumin, 0.05% Tween-20 in PBS for 2 h. Calf thymus double stranded DNA (ctDNA) was sourced from Worthington Biochemical Corporation (cat# LS002105), resuspended in TE buffer (Tris 10 mM, EDTA 1 mM, pH 8.0), and extracted several times with phenol:chloroform:isoamyl alcohol (25:24:1; Millipore Sigma cat# 77617) and chloroform:isoamyl alcohol (24:1 Millipore Sigma cat# 25666). ctDNA was diluted in 1X SSC (150 mM NaCl, 15 mM Na citrate, pH 7). The anti-DNA antibody Val-1205 is a humanized and further modified version of the lupus mouse monoclonal 3E10 developed by Valerion Therapeutics (stock number VALE-915) and kindly provided by Drs. Robert Shaffer and Dustin Armstrong to co-author Dr. David Pisetsky. This primary antibody was typically used at 200 ng/mL and the secondary antibody linked to horseradish peroxidase was used at 1:2000 [anti-human IgG, gamma chain specific, conjugated to peroxidase (Millipore Sigma cat# A6029)]. As needed, antibodies were diluted in 0.1% bovine serum albumin, 0.05% Tween-20 in PBS. Peroxidase activity was assessed by incubation with the peroxidase substrate 3,3′,5,5′-Tetramethylbenzidine dihydrochloride or TMB (Millipore Sigma cat# 860336) for 30 min, and the reaction stopped by the addition of 2 M sulfuric acid. Absorbance of each well was read at 450 nm using a Molecular Devices Spectra Max i3 plate reader and associated SoftMaxPro 6.3 software.

Polymer capture ELISAs

The ability of polymers to bind DNA was assayed by a modified sandwich ELISA composed of plate bound polymer incubated with a dilution series of ctDNA followed by the anti-DNA antibody Val-1205. Polymers were prepared in PBS at 1 μg/mL (solution pH 7.1), directly bound to microtiter plates, incubated with calf thymus DNA of various dilutions (ranging from 0.003 ng/mL to 1000 ng/mL), and the efficiency of DNA capture gauged by the signal arising from binding of the anti-DNA Val-1205 antibody (200 ng/mL).

Polymer blocking, competition and displacement ELISAs

The ability of polymers to compete with the anti-DNA antibody Val-1205 for the binding of DNA was assayed by ELISA. Microtiter plates were incubated overnight with calf thymus DNA at 5 μg/mL in 1X SSC. The polymers were prepared in ELISA dilution buffer and associated pHs modestly rose with polymer concentration but remained similar to one another: for instance, at 12.5 μg/mL the solution pHs were 7.2, and at 200 μg/mL the solution pHs were 7.5. For the blocking assay a polymer dilution series from 1600 μg/mL to 0 μg/mL was incubated with the DNA for 1 h prior to addition of the Val-1205 antibody (400 ng/mL, 200 ng/mL final), incubated jointly for 1 h, washed and then incubated with the secondary antibody. For the competition assay the same polymer dilution series as above was added together with the Val-1205 antibody (400 ng/mL, 200 ng/mL final) for an incubation period of 1 h, washed and then incubated with the secondary antibody. For the displacement assay, the Val-1205 antibody (400 ng/mL, 200 ng/mL final) was added to the plate for 1 h prior to the addition of the polymer dilution series, incubated jointly for 1 h, washed and then incubated with the secondary antibody.

Cell toxicity assays

HEK-Blue hTLR 3, 4, 7, and 9 cells were plated for toxicity assays in 96-well plates at 40,000 cells per well and allowed to settle overnight at 37°C in 5% CO2 at 95% relative humidity. Media were then removed and fresh media with varying concentrations of polymer in 100 μL total volume were added and allowed to incubate. Associated pHs of the culture media rose with polymer concentration, similarly for all the polymers tested: for instance, at 16 μM the solution pHs were 7.6, at 64 μM the solution pHs were 7.9, and at 256 μM the solution pHs were 8.3. The CellTiter-Glo® luminescent cell viability assay was purchased from Promega and prepared according to manufacturer's instructions at time of assay. After 24 h, 100 μL of CellTiterGlo reagent was added to each well and contents mixed on an orbital shaker for 2 min and then incubated at room temperature for 10 min. The luminance of the wells was read on a Spectramax i3 (Molecular Devices) plate reader and data presented as percent of luminance for cells alone without added polymer. Data are the combined means of the 4 cell lines tested, with three technical replicates averaged to generate the data point for each cell line.

RAW 264.7 cells were plated for time course toxicity assays in 96-well plates at 7,000 cells per well and allowed to settle overnight at 37°C in 5% CO2 at 95% relative humidity. Media were removed and replaced with fresh media with varying concentrations of G3 or G3 50:50 polymers in 100 μL total volume added and allowed to incubate. Media pH increased uniformly as polymer concentrations increased, as described above for the HEK studies. The CellTiter-Glo® luminescent cell viability assay was purchased from Promega and prepared according to manufacturer's instructions at time of assay. At 24, 48, and 72 h, 60 μL of CellTiterGlo reagent was added to each well and contents mixed on an orbital shaker for 2 min and then incubated at room temperature for 10 min. The luminance of the wells was read on a Spectramax i3 (Molecular Devices) plate reader. Data are the average of three technical replicates and presented as percent of luminance for cells alone without added polymer.

General notes on the studies in mice

No power calculation was used to determine group sizes; group sizes were determined by logistical feasibility and experience of authors gained from earlier studies. Histological scoring was completed in a masked fashion by a veterinary pathologist (J.I.E.).

Short term toxicity studies in mice

Short-term toxicity was assessed over three studies under a repeated protocol but with varied polymers and doses. Female C57BL/6J mice received intraperitoneal injections of saline or 20 or 40 mg/kg of selected dendrimer polymers: PAMAM G2, G3 50:50, G3, G4 50:50, or G4 every three days for 4 total doses. Mice were evaluated and weighed daily and sacrificed 24 h after final injection. At sacrifice, blood was collected for complete blood count and serum prepared for liver and kidney function tests and quantitation of inflammatory markers. Necropsy was performed at time of death by a veterinary pathologist and organs were weighed and fixed in 10% formalin and processed as FFPE samples for H&E staining. Livers were assessed for hepatic surface inflammation based on pleocellular infiltration of neutrophils, macrophages, and lymphoid cells. Kidneys were scored for protein droplet accumulations and for nephropathic changes on a semi-quantitative score of 0–4 with zero being normal kidney and 4 being the most severe change. Protein droplet scores were based on relative number and size of droplets and number of tubules involved. Nephropathy scores were based on % cortex involved as well as the degree of tubular epithelial change involving basophilia and regenerative hypertrophy and hyperplasia. Scores ranged from 0 (normal), 1 (minimal), 2 (mild), 3 (moderate), through 4 (severe). Serum chemistry tests were performed by IDEXX labs. The first study involved all polymers at both doses (20 mg/kg and 40 mg/kg) and used 4–5 mice per treatment group; the second study, done in conjunction with the "Recovery Study" described below, involved 40 mg/kg dosing of all polymers and used 4 to 5 mice per treatment group; the third study focused on G3 and G3 50:50 polymers and used 5 to 7 mice per treatment group. Numbers of animals in each group do show variability dependent on the particular assay: weight assessment, reflecting the numbers of mice at the start of the treatments, has the highest n; the histological analyses show a modest dropoff in numbers as the occasional animal expired during the study; and serum chemistry numbers are lower because serum was not acquired in all contexts, notably for the recovery mice described below.

Analysis of inflammatory cytokines using LEGENDplex

Quantitation of mouse cytokines in serum obtained from mice in the final short term toxicity study described above was accomplished using the LEGENDplex™ Mouse Anti-Virus Response Panel

(BioLegend) and the associated LEGENDplex™v8 Data Analysis Software. Each serum sample was diluted 1:1 and then assessed in two wells. The assay and acquiring of the flow samples on a Beckman Coulter CytoFLEX flow cytometer followed the detailed instructions provided by the manufacturer's LEGENDplex™ manual.

Recovery Study in mice

To assess for transience of polymer-induced inflammation and kidney lesions, the above study's protocol was repeated with G2, G3, G3 50:50 and G4 50:50 dosed at 40 mg/kg, with the mice left untreated after final dosing for two additional weeks before sacrifice. Five mice per group were treated with 4 doses of polymer or saline, and weighed every other day for two weeks following final treatment, and then sacrificed with dissection of the liver, kidneys, and diaphragm from each mouse and processed as FFPE samples for H&E staining.

SLE long term treatment

Female and male MRL-*lpr* mice were weighed and received intraperitoneal injections of PAMAM-G3 (20 mg/kg, Nf = 23, Nm = 16), PAMAM-G3 50:50 (40 mg/kg, Nf = 21, Nm = 22), PAMAM G4 50:50 (40 mg/kg, Nf = 13, Nm = 18), or saline (Nf = 29, Nm = 29) twice per week; in the case of females for a period of 9 weeks starting at 9 weeks of age and in the case of males for a period of 10 weeks starting at 10 weeks of age. Mice were then sacrificed, and citrated plasma and tissue were collected for further analysis. For analysis of kidney disease, kidneys were collected and further processed as FFPE samples for H&E staining. Glomerulonephritis in the MRL-*lpr* mice was scored based on glomerular hypercellularity and thickening of glomerular basement membranes. Lymphoproliferative changes and tubular changes were not scored as part of the lupus assessment. Glomerular change was scored from 0 (normal), 1 (minimal), 2 (mild), 3 (moderate), through 4 (severe).

QUANTIFICATION AND STATISTICAL ANALYSIS

Table S1 documents the statistical analyses used in the study. Much of the information as to the test used, n, and error, is also presented in the associated figure legend. For continuous data, one-way ANOVA, two-way ANOVA, mixed-effects models, and IC50 determinations were performed using GraphPad Prism v9.4.1. Significant ANOVAs were followed by Tukey's post hoc test for comparison of all groups to one another and mixed-effects models were followed by Dunnett's post hoc test for comparison of polymer groups to saline treated contols. Analysis of ordinal tissue score data arising from the toxicity studies in C57BL/6J females and from the treatment studies of lupus prone MRL-*lpr* females and males was guided by Meyerholz et al.,[36] and used GraphPad Prism v9.4.1. The Kruskal-Wallis nonparametric test was applied to determine whether any treatment group median was different from the others. Upon evidence for difference, post hoc evaluations using the Dunn's multiple comparisons test were performed. For the toxicity studies, the comparisons generally compared all groups to one another. However, when comparing particular dosage or washout effects for each particular polymer, multiple Mann-Whitney tests with a false discovery rate set to 1% were employed with q values (false discovery rate adjusted p values) indicated. For the SLE treatment study of MRL-*lpr* mice, comparisons were made with respect to the control saline mice treatment group. For all tests, *$p < 0.05$, **$p < 0.01$, ***$p < 0.001$, and ***$p < 0.0001$.